THE EFFECT OF EXTERNAL CONTROLS ON CHANNEL-BELT STACKING PATTERNS IN THE FLUVIO-DELTAIC DOMAIN OF A LANDSCAPE FLUME

Louisa Tlili

Supervisor: Dr. Joris T. Eggenhuisen

Second supervisor: Jochem Bijkerk

Msc Thesis ● Faculty of Geosciences ● Utrecht University

15/08/2013

Abstract

External controls such as glacio-eustatic sea-level variation are known to have a strong influence on the areas of deposition and erosion, thereby affecting the location of channels, as well as their stacking patterns. Recent studies have shown that paleo-environmental (allogenic) signals preserved in stratigraphy may be overprinted by internally generated (autogenic) sedimentation. However, it is unclear to what affects external controls, such as sea-level change, subsidence, but also sediment mixture may have on the time scale over which there is a transition between allogenic and autogenic stratigraphy. Two sets of experiments were carried out in the Eurotank Flume Laboratory at Utrecht University during which the morphology and the topography of the fluvial system were regularly monitored to determine compensational stacking. Using statistical methods, basin filling trends were quantified. The compensation index (σ_{ss}) and the compensation time scale (κ_n) were used to explore how compensation, the tendency for sediment transport to preferentially fill topographic lows, varies over the basin´s length. The observed compensation time scale, which was defined as the break in the basin-filling trend, varies depending on whether there are any sea-level changes. The time scale at which the fluvial system becomes fully compensated will decrease from source to sink with no sea-level change, but increase during sea-level fall. Understanding channel migration and the resulting channel stacking patterns is important as it provides additional insight in deltas as hydrocarbon reservoirs, and enables further study as to how deltas and continental margins prograde.

Contents

1. Introduction

Channels are landforms, the geometric entities that transport water and sediments, which are not directly observable in the stratigraphic records (Blum et al. 2013) but their behaviour is important in understanding the behaviour of a sedimentary succession through time.
Channel fills form over years to centuries for neck cut offs, and decades to millennia for avulsions (Blum et al. 2013). Reproducing quantitative stratigraphic models as the internal dynamics of depositional systems may be complicated as they entwine with external boundary conditions that control basin sedimentation (Wang et al. 2011). Muto et al. (2007) defined the term 'autogenic' as a response to steady external forcing and 'allogenic' as a response to non-steady external forcing. Differentiating between these allogenic signatures (externally driven) from autogenic variations (internally generated), is key to correctly understanding paleo-environmental variations in sedimentary records (Powell et al. 2012).
Flume experiments provide a controlled environment, in which, channel stacking patterns can be studied much more easily and comprehensively than in nature (Paola et al. 2009). Such experiments yield stratigraphic responses to allocyclic forcing that are remarkably similar to those in real-world prototypes, hinting at scale independency with strong dependence on boundary conditions but weak dependence on the actual sediment transport dynamics (Postma et al. 2008) allowing the study of geological processes lasting >100 kyr within weeks. This provides better understanding of large-scale stratigraphy and morphodynamic responses as well as how to separate allogenic and autogenic signatures in the rock record (Powell et al. 2012). Understanding channel migration and the resulting channel stacking patterns with respect to basin depth and sea-level change is important because it provides additional insight in deltas as hydrocarbon reservoirs, and allows to study in detail how deltas and continental margins prograde.

Aim

Straub et al. (2009) suggested to further analyse changes in compensation index with allogenic forcings as it would provide a valuable next step in understanding the connection between autogenic and allogenic processes in stratigraphy.

This study aims to obtain a better understanding on channel-belt stacking patterns along the fluvio-deltaic domain by (1) looking at how compensation varies with time and (2) defining a compensation time scale which predicts when the transition from autogenic to allogenic deposits differs during sea-level change, subsidence and sediment composition. This will be done through two sets of landscape flume experiments at Utrecht University

2. Theoretical analysis

Compensation stacking

Compensational stacking has been used to describe large-scale architecture in deep-water, fluvial, and deltaic packages (Mohrig et al. 2000). It is the tendency of deposits to preferentially fill topographic lows, smoothing out topographic relief by “compensating” for localised deposition from discrete depositional elements (Straub et al. 2009) whilst minimizing potential energy associated with elevation gradients (Mutti and Normark 1987; Stow and Johansson 2000). According to Wang et al. (2011), depositional elements cluster to form anti-compensationally stacked deposits, while over long time intervals, deposit complexes stack in purely compensational manner. In the fluvio-deltaic domain, external controls such as glacio-eustatic sea-level variation and lateral variations in the depth of the receiving basin are known to have a strong influence on the areas of accommodation and deposition (e.g. Posamentier et al. 1988), therefore strongly affecting the location of channels, as well as their stacking pattern.

Compensation index

Straub et al. (2009) developed a practical and readily applicable measure for the degree of compensation in sedimentary deposits. This statistical compensation index measures the tendency of marine and terrestrial depositional systems to fill basins through compensational stacking (Straub et al. 2009).

Through studying the transition in alluvial depositional geometry from morphologies controlled by local channel geometry to morphologies controlled by regional sediment supply and accommodation, Sheets et al. (2002) proposed that the deposit thickness (i.e., time) required to make this transition could be scaled to the time necessary for the fluvial system to occupy every spot in the basin several times, therefore averaging out local autogenic effects and bringing the geometry of the long time scale depositional geometry in balance with accommodation (Fig.1) (Sheets et al. 2002).

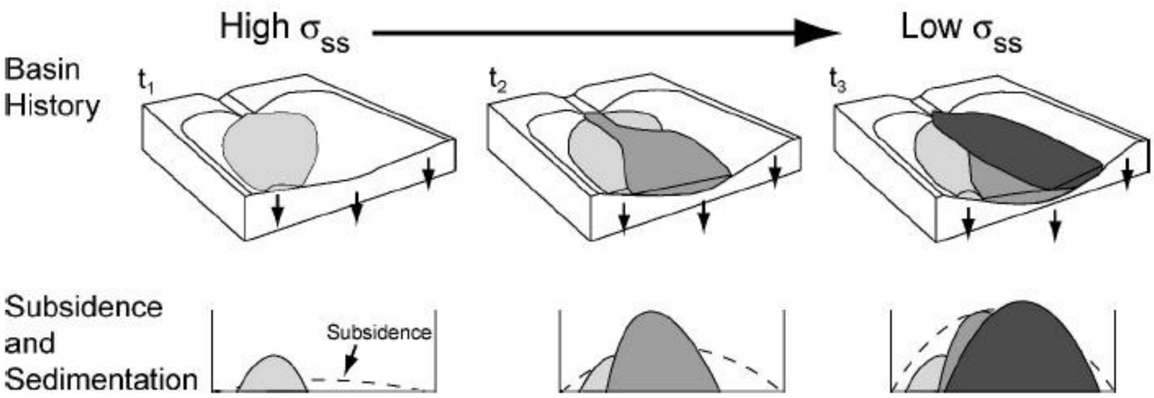

Figure 1: Schematic from Lyons (2004) describing the progression of a basin towards equilibrium. The balance between sedimentation and subsidence in a basin improves over time. In the block diagrams illustrating basin history, subsidence (indicated by arrows) is temporally constant but spatially variable. Sedimentation, represented by lobes of different colour is both temporally and spatially variable. The balance between sedimentation and subsidence for an arbitrary cross section at the three time steps is represented graphically below each block. At the earliest time, t_1, subsidence is small and sedimentation is local resulting in a poor fit between the two. However, as the basin develops, subsidence increases and the sedimentary system has an opportunity to occupy a larger fraction of the total area. The result then, at later times t_2 and t_3, is that the fit between sedimentation and subsidence improves. Taking the ratio of sedimentation over subsidence pointwise across the basin for each time step would produce a ratio of distribution with decreasing standard deviation over time (Straub et al., 2009).

Over short time scales, deposition in a basin is controlled by the type of transport system which results in an increase in the sedimentation variability at any one point within the fluvial system when compared to higher time scales (Straub et al. 2009).
However, Sheets et al. (2002) do not comment on the time needed for this transition to occur, so Straub et al. (2009) used their data to examine that problem and to illustrate how the variability in sedimentation (σ_{ss}) against time can be used to measure the tendency of deposits to stack via compensation. Their method used the decay of σ_{ss} between selected depositional horizons with increasing vertical stratigraphic averaging distance:

$$\sigma_{ss}(T) = \left\{ \int_L \left[\frac{r(T;x)}{r\hat{}(x)} - 1 \right]^2 dL \right\}^{1/2}, \qquad (1)$$

where *r(T;x)* is the local sedimentation rate measured over a stratigraphic interval *T*, *x* is a horizontal coordinate, *L* is the cross-basin length, and *r^(x)* is the local long-term sedimentation (or subsidence) rate. The value of σ_{ss} serves as a measure of the extent of subsidence control in a basin.

Straub et al. 2009, showed that σ_{ss} decays as a power-law function of measurement time window,

$$\sigma_{ss} = aT^{-\kappa} , \qquad (2)$$

where the exponent, κ, was termed the compensation index, and *a* is a leading coefficient in the power-law. The compensation index κ was found theoretically to be 0.5 for random stacking that is uncorrelated in space and time, and 1.0 for perfect compensational stacking (note that "random" refers to the mean probabilistic processes that have no detectable correlation in time.) Values <0.5 indicate anti-compensation (Fig.2).

Straub et al. (2009)'s 1D models suggest that the tendency of deposits to stack compensationally can be measured through the decay of σ_{ss} with time. Specifically, the decay of σ_{ss} for natural basins should follow a power-law trend and have compensation index (κ) values between 0 and 1.0, with these end-member values representing persistence (anti-compensation) which shows an increase in the depositional topography, and perfect compensation, respectively (Straub et al., 2009).

The end member κ = 0 is unlikely to occur in nature, however, low κ value suggest persistence in deposition trends as indicated for example in multi-story channel sand bodies (e.g., Jerolmack and Paola, 2007).

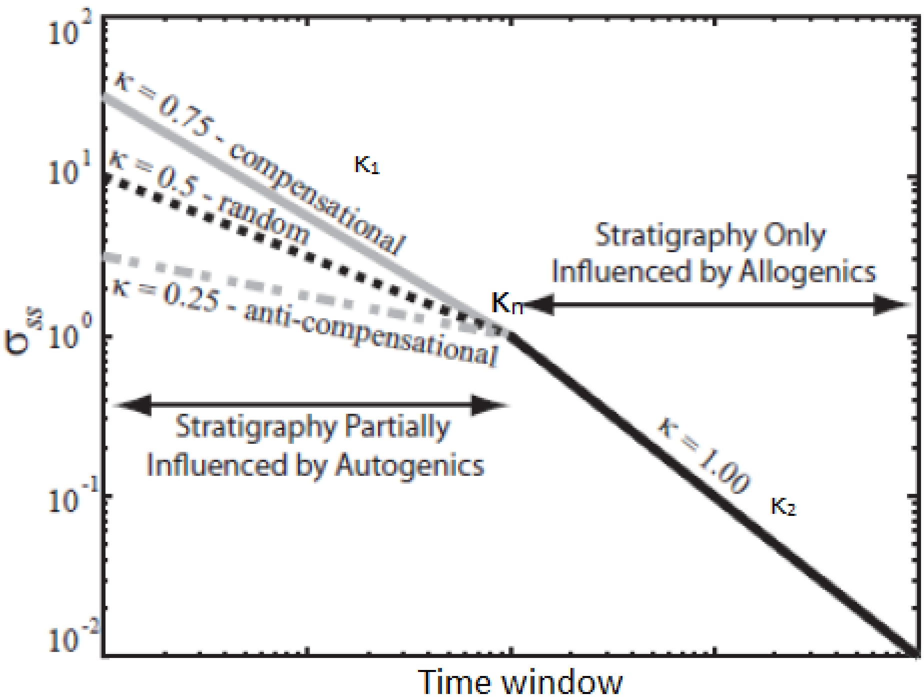

Figure 2: Decay of σ_{ss} as a function of time for three hypothetical basins. (modified from Straub and Wang 2013).

For all basins, the decay of σ_{ss} with time is characterized by a κ_2 equal to 1 at time scales greater than κ_n (also referred to as T_c in Wang et al. (2011) and Straub and Wang (2013), κ_n represents the neck-point). Basin filling during κ_2 is only influenced by allogenic forcings. Before κ_n, fluvial systems are characterized by stochastic autogenics of varying magnitude and thus, varying κ_1. Wang et al. (2011) found that the time scale at which κ_2 becomes fully compensational represents a shift from stratigraphy that partially records stochastic autogenic processes to stratigraphy determined purely by regional sediment supply and accommodation. They also demonstrated that the measurement window can be spatial, suggesting that stratigraphic horizons may be used in place of timelines for analysis of deposits that are missing adequate age control (Wang et al. 2011).

Past findings

Since the original fuvial architecture model of Leeder (1978), in which, the connection between avulsion and the architecture of channel sand bodies was first recognised, a great deal of research was done to develop the connection in two and then three dimensions. Leeder (1978) assumed the channel positions to be random and independent of previous channel locations. Allen (1979) proposed that abandoned channels would remain high for a time, leading to avoidance of previous channels and an overall tendency to distribute channel bodies more compensationally than in Leeder's model. Apart from major developments in field tests, incorporation of avulsion-architecture into sequence stratigraphy, refinement of understanding avulsion mechanisms and proposals of characteristic avulsion-related stratigraphic patterns, Jerolmack and Paola (2007) developed a cellular channel model in which relict channels served as attractors until they were filled with sediment, leading to the development of multi-story channel bodies.

Hierarchical levels

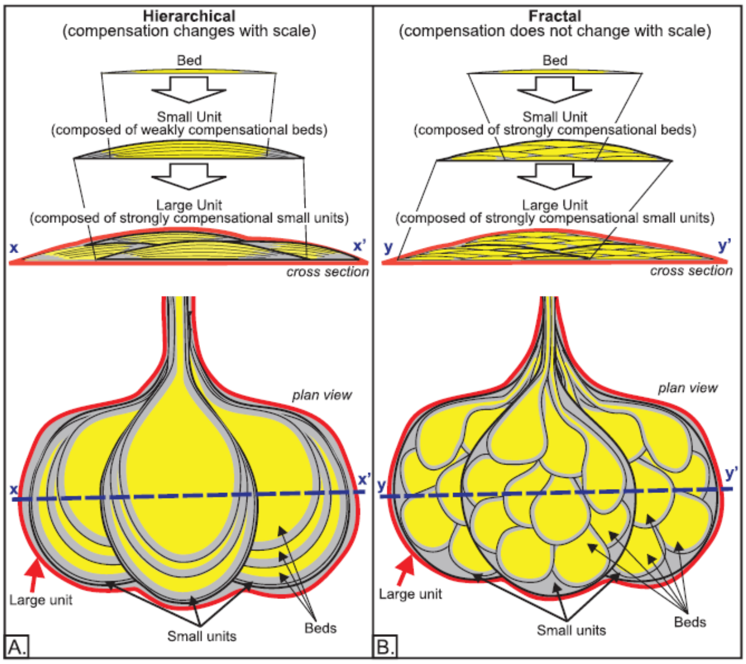

Figure 3: A) Diagram of hierarchical, scale-dependent, compensation whereby large units stack more compensationally than small units (no scale implied). Yellow represents sand-rich strata and grey represents mud-rich strata. B) Diagram of fractal, scale-invariant, compensation whereby compensation does not change with scale.

Straub and Pyles (2009) argued that if compensation were fractal; bed, stories and elements would share similar κ_{CV} (coefficient of variation) values as small-(bed) and large-scale (elements) units would stack similarly (Fig. 3). However, they noticed different decay values for each hierarchical levels with an increase in compensation along a longitudinal transect through the distributive submarine fan, thus justifying hierarchical divisions based on compensation. Furthermore, they proposed that bed-scale stacking in channel elements is influenced by the size of flows and the width of the channel whereas bed-scale stacking in lobe elements is influenced by focusing from the updip, genetically related channel, meaning that while lobes have no lateral boundary condition (i.e., channel walls) the location of the sediment transport fields laterally constrained, or focused, by the fixed updip channel that that feeds sediment to the lobe element (Straub and Pyles 2012). Element-scale stacking appears to results from processes such as avulsion, which have a longer time and space scale than bed- and story-scale stacking patterns, and are possibly influenced by different systems (Straub and Pyles 2012). These properties could include allogenic forcings such as frequency of flow events, long-term sedimentation supply, subsidence rate, and the size and shape of the basin and/or autogenic processes including super-elevation and the development of lateral slopes of the channel-lobe element due to sedimentation (Straub and Mohrig 2008; Prelat et al. 2010; Macdonald et al. 2011).

These scale-dependent dynamics are imprinted in the stratigraphic record and quantitatively manifested as the punctuated shifts in κ_{CV} with time scale (Straub and Pyles 2012). The increase in κ_{CV} with hierarchical scale also indicates an increase in stratigraphic organization with scale as κ_{CV} values near 0.5 indicate random stacking patterns, while κ_{CV} values near 1.0 represent organized stacking of deposits with pure compensation (Straub et al. 2009). By classifying compensation as hierarchical, stratigraphy could be grouped into hierarchical units to captures natural structure.

3. Methods

To examine the effect of external controls on channel-belt stacking patterns, four physical laboratory experiments were carried out from the 5th of March until the 30th of May 2013. While directly up scaling experimental systems to field scale systems remains challenging, the existence of scale independence in some aspects of sediment transport and morphodynamics allows experimental systems to produce spatial structure and kinematics that, although imperfect, compare well with natural systems. As a result, these experiments provide morphodynamic and stratigraphic insight into the evolution of channelized settings under an array of external and internal influences (Straub and Wang 2013).

Experimental design

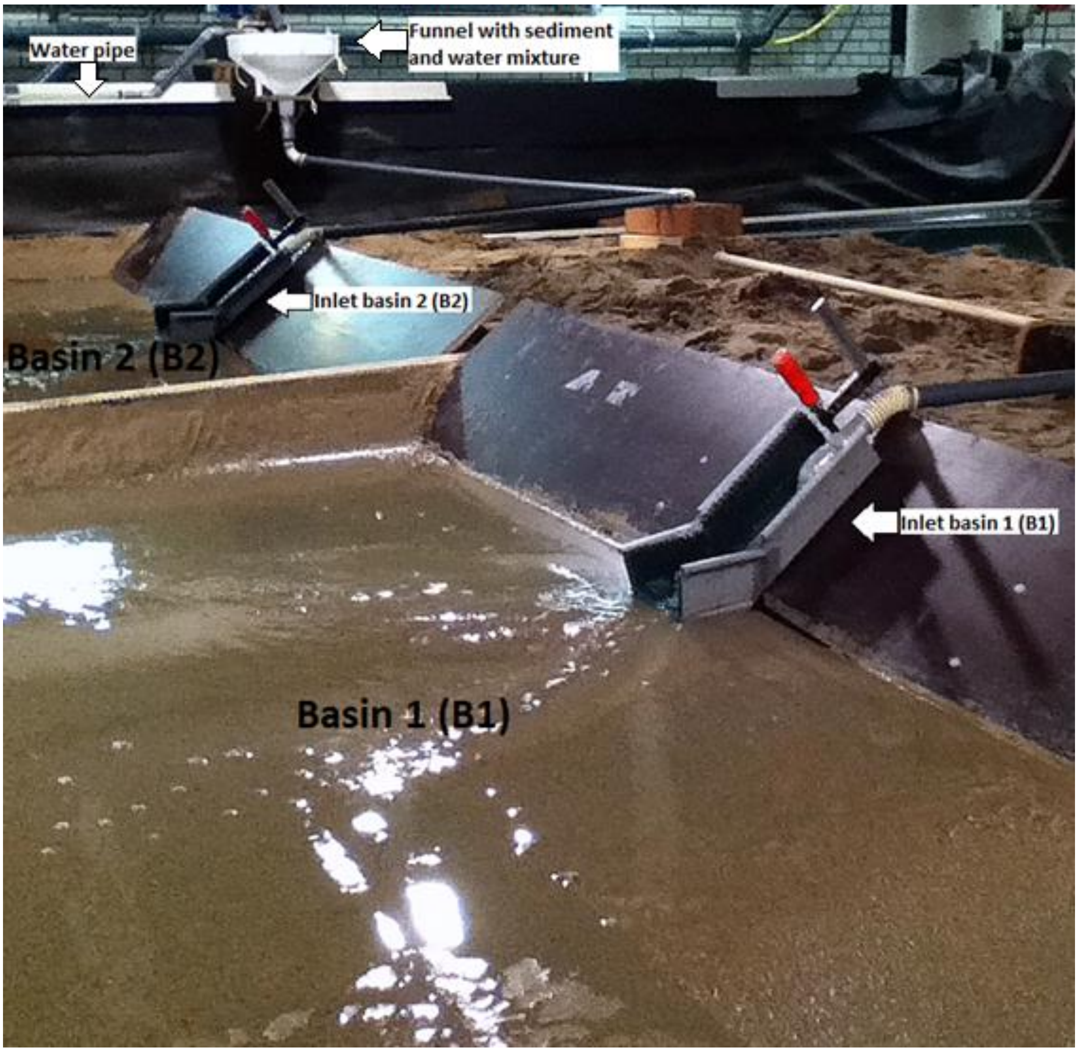

Figure 4: Experimental setup

Two sets of experiments were carried for which the setup consisted of two rectangular ducts serving as fluvial valleys, shelf, slope and basin. Sediment and water discharge were mixed in a funnel and fed from a single mobile inlet source upstream (Fig.4). Water discharge was 1000L/hr and sediment discharge was 4L/hr.

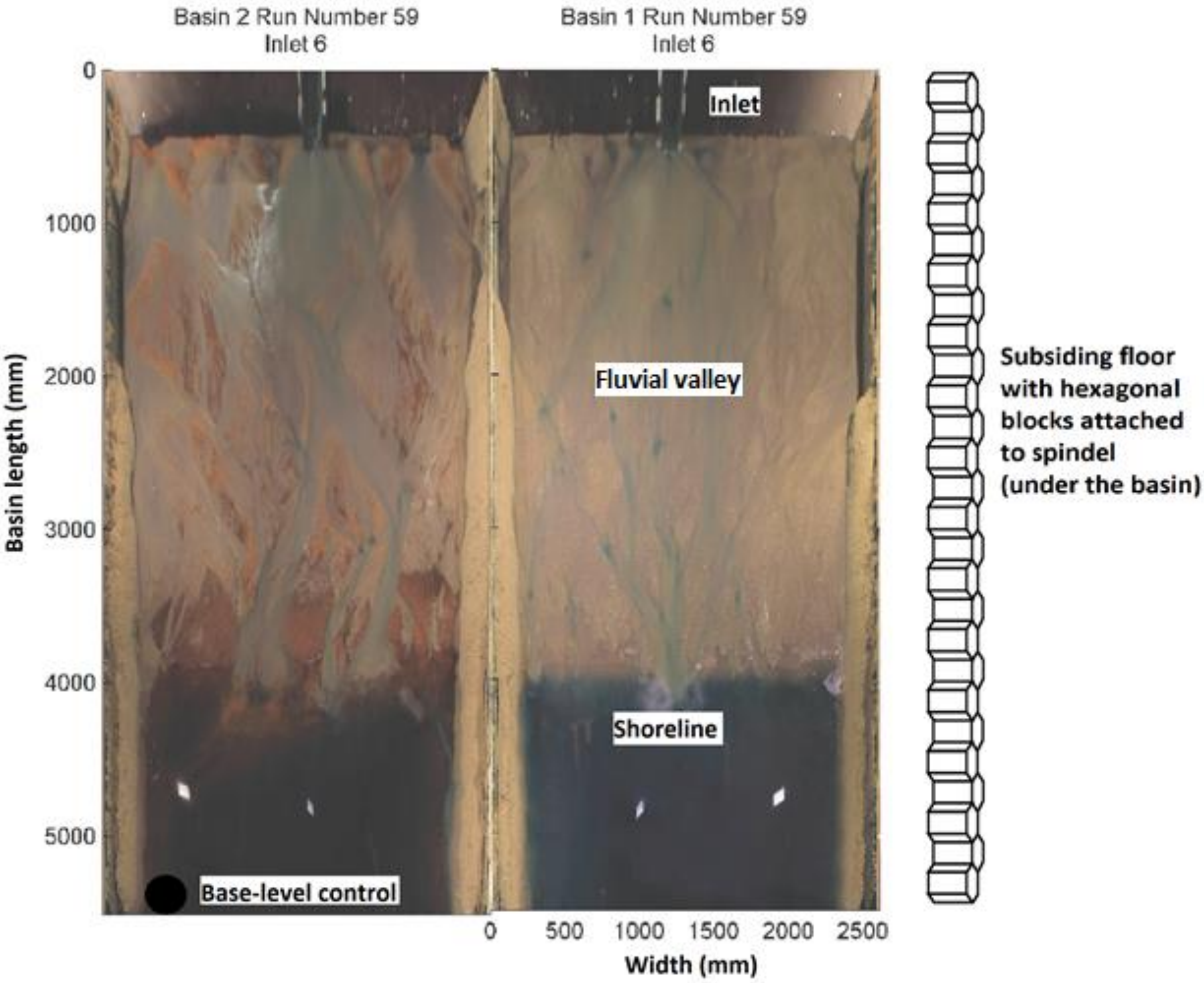

Figure 5: Top view of the setup

A height-adjustable overflow controlled sea-level and, a system of moveable hexagonal blocks attached to spindles located under the experimental setup controlled subsidence (Fig.5). Unlike other experimental research in the same field, a rectangular shaped basin from source to sink was used with a moveable inlet along the upstream boundary. Two sub-experiments were investigated during each experiment. The flume was separated by a side-wall in the middles, in order to create to independent basins.

Experiment one (Exp1)

The initial topography of both basins was, more or less identical. Basin 1 (B1) and basin (B2) were mirror images of each other in terms of their inlet positions. The inlet position randomly changed at the end of every run which lasted 30 minutes. Exp1 had sand-walls on the side of the fluvial valley to minimize incision against the walls and direct the channels away from the sidewalls. There were 12 possible inlet positions, each of which was right next to the other.

In terms of their setup, the two basins of Exp1 were slightly differing. B1 had an input of solely, sand, whilst, B2 had a sediment mixture composed of 67% sand and 33% crashed walnut shell (of which 50% was medium sized grains, 25% was fine grains and 25% was coarse grains). The sediment discharge in both basins was identical. The walnut-shells are substantially more mobile than the sand grains and serve as a proxy for fine-grained clastics.

In order to visualize the active channel network, the input water was dyed with blue paint. The water discharge in B1 was fresh water whilst the discharge in B2 was salt water (the salt mixture was done by adding table salt in the water tanks until a salinity of 40‰ was reached) to promote subaqueous transport of the crushed walnut-shell. To prevent the salt water from replacing fresh surface water, fresh water was added directly to the basin, generating a fresh water lid, while the overflow drained only the deep, salt water fraction at the bottom of the basin, thus promoting deep water circulation.

Experiment two (Exp2)

The initial topography of the fluvial system was identical, but, B2 started with a fully subsided deep basin whilst the deep basin of B1 was gradually subsided at the end of every 10 runs.

Experimental procedure

Experiment one (EXP1)

Exp1 had an initial build-out phase to create a natural profile of 56 runs (28hours). The recorded experiment lasted 115 runs (57.5hours) during which, no changes were brought to the system.

Experiment two (EXP2)

Exp2 had an initial build-out phase of 34 runs (17hours). The recorded experiment lasted 180 runs (90hours) during which sea-level was adjusted every 15minutes (Fig. 6).

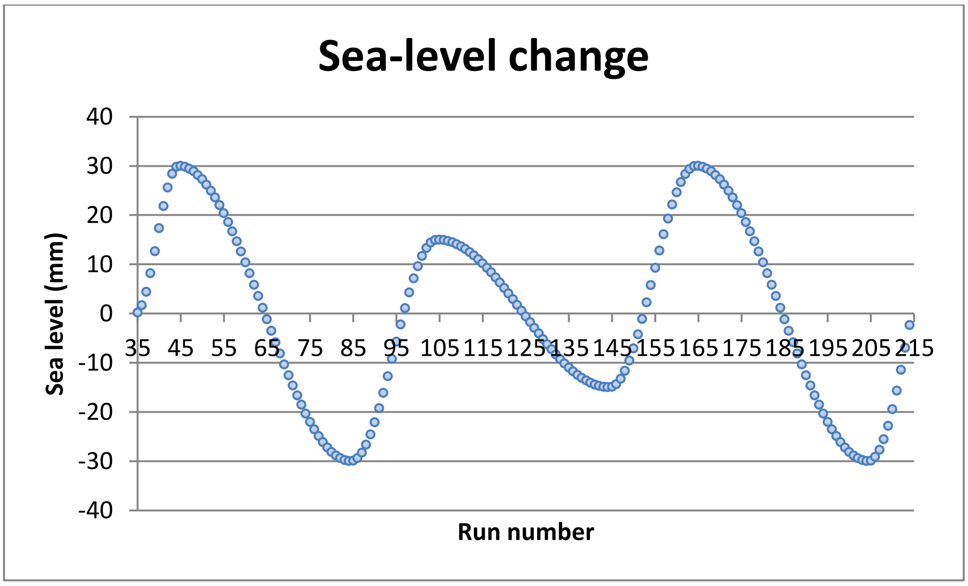

Figure 6: Sea-level variation curve of EXP2

The sea-level curve represents an eccentric curve lasting 100kyrs.

At the end of every run (in both EXP1 and EXP2), the sea-level was dropped below the shelf-edge to measure the topography of the entire top-set at the end of each run. The sand-walls from EXP1 eventually washed away starting upstream and as there were only 12 inlets, which were focused in the centre of the fluvial system, sediment supply became less focused along the sand-walls, thus increasing the topography in the central and upstream area of the basin causing channels to preferentially flow towards the sidewalls. For those reasons, Exp2 was executed without any sand-walls and the inlet number was increased to 13.

Both basins (B1 and B2) of Exp2 had a sediment mixture composed of 75% sand and 25% crashed walnut shells (of which 50% was medium sized grains, 25% was fine grains and 25% was coarse grains). The sediment discharge in both basins was identical.

The goal of the experiments was to create a self-organized system which can be monitored in detail over special and temporal scales which are impossible to obtain in the field. In order to achieve that, three types of data were collected from the experiment: system morphology, surface topography, and deposit stratigraphy. (1)The morphology of the fluvial system was recorded with two cameras CANON 1100D (one for each basin) which took snapshots of the basin every minute. (2)Topographic measurements of the fluvial system were taken with a scanning laser at the end of each run (every 30 minutes). The basin was drained at the end of every five runs and a scan was done to record subaqueous topography. (3)Photographic lacquer peels were used for the deposit stratigraphy.

An event on a morphology image could be located, matched with the elevation data from the same point on the corresponding topographic image as well as with the same point on the lacquer peel photograph thus, providing three-dimensional (3D) information of the basin.

Scaling

In this physical experiment, only geometries are considered as analogues of natural systems since sediment properties and hydrodynamic conditions cannot be scaled. This model focuses on the succession of stratal patterns, and not on the simulation of sediment transport (Paola et al., 2009).

Errors in the experiments and analysis

Uncertainties caused during the experiments

The sediment feeder of B2 (a calibrated screw feeder which released the sediment is the flume at an adjustable speed) was found to have slightly changed by the end ofEXP1. Although the difference was minor, it is important to note that, at some point of the experiment, B2 received less sediment discharge compared to B1. At the start of every run, water discharged was checked to make sure that it was constant and equal between the two basins however, it is important to note that, in natural systems the ratio of water discharge to sediment discharge does not always stay constant. In natural basins, these parameters vary over many time scales which could confound the interpretation for both allogenic and autogenic signals. For example, larger water discharge explicitly changes the allogenic forcing, but also makes larger channels and therefore alters the time scales of autogenic dynamics (Wang et al., 2011).

Two motors were inserted in each water tank, so the salt could be dissolved and circulated constantly during the experiments. The saltiness of the water was also checked every few runs to make sure it maintained a salinity of approximately 40‰. The proportion of walnut shell was measured each time using 1000ml beakers in order to obtain the best accuracy.

A timer was set, so as not to forget to change the sea-level every 15 minutes.

For the topography scan, a few minutes were waited so that the water that was still present on the top-set, could be absorbed, this was to ensure that there would be no reflections during the laser scan. However, there were some scour holes in which water remained.

Some errors resulted when water started escaping from the sidewall, resulting in incision along the side right side of EXP1-B2 during R157.

Another error was when the laser scan did not complete its scan of B2, and a few lines were missing. Fortunately, the scan of that particular basin was not needed as only topography of B1 during EXP2, was checked for after we had subsided it.

Pictures of the empty basin of EXP2 at the end of R089 and the entire R109 of EXP2-B2 are missing.

After B1 of EXP2 was subsided overnight, we would check the spindles to make sure every block had been subsided properly, as the robot did not always work.

Finally, the last source of error was due to the spindle robot. After the equilibrium run for EXP2, B2 was fully subsided, unfortunately, some of the blocks got stuck during subsidence so after manually lifting them and dropping them, they would get unstuck. This problem might have also occurred in B1, but because the deep basin was gradually subsided, it was harder to determine whether or not, the block did freeze. Fortunately, the topographic scans of the drained basin prior and after subsidence enabled possible comparison.

Uncertainties caused during the analysis

In the erosion deposition models, a few figures had some error lines. This probably resulted from power shortages during the scan.

4. Results

Development of the basin

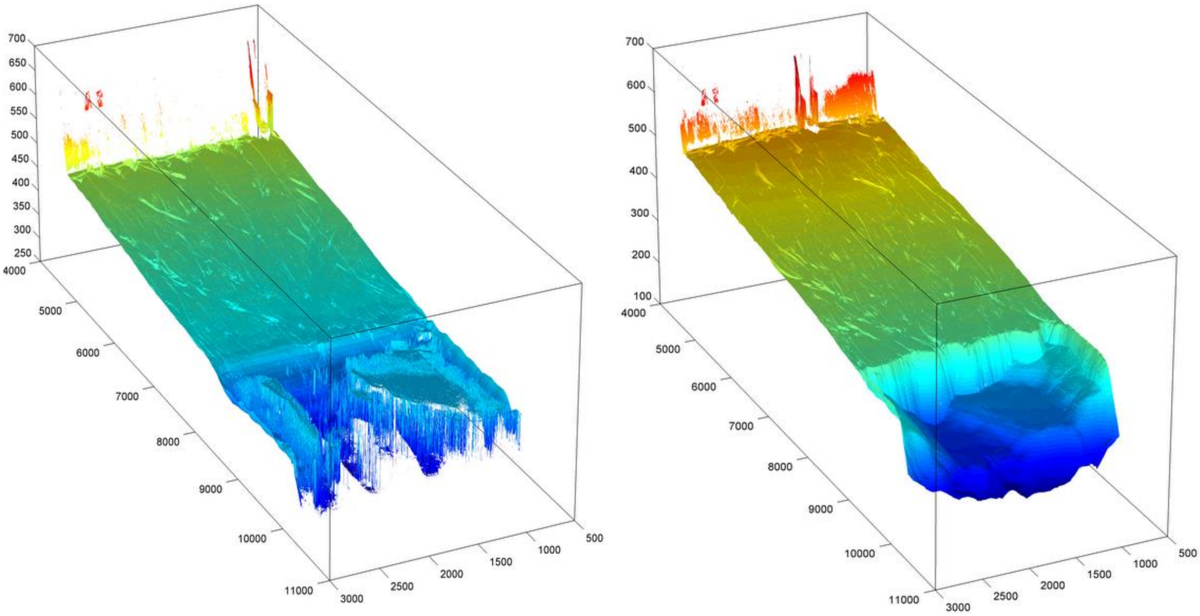

Figure 7: EXP1 3D scan of B1 at R057 (the start of the experiment) and R171 (the end of the experiment), respectively

Figure 7, shows that the basin has significantly prograded and aggraded with time when the basin had a constant discharge and no sea –level change changes. Aggradation of the system resulted from the transport and deposition of sediment by migrating channelized flow. For that reason experiment 1 (EXP1) basin 2 (B2) will act as the control experiment for the study.

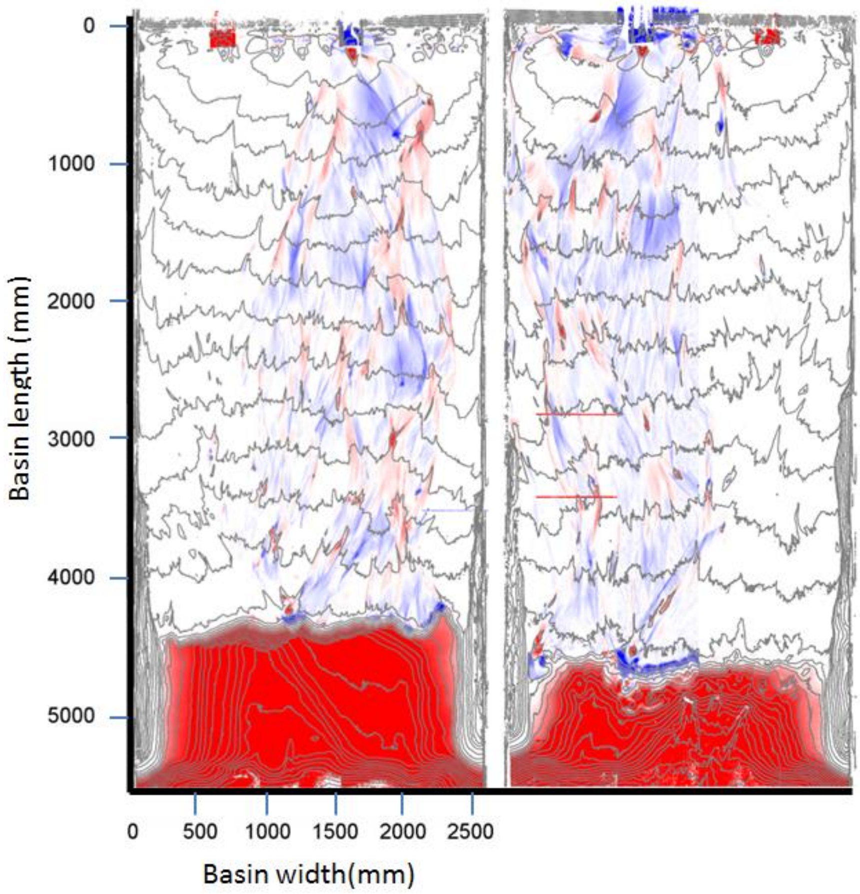

Figure 8: EXP1 Aggradation of B1 and B2, respectively at R171

B2 (sand-walnut mixture) shows that, even though the external conditions were the same as B1(solely sand), the basin aggradated much further than B1, suggesting that a combination of walnut mixed with sand and salt water, improved sediment transport along the fluvial system. There appears to be a uniform increase of the fluvial system with no observed preferance for deep or shallow basin.

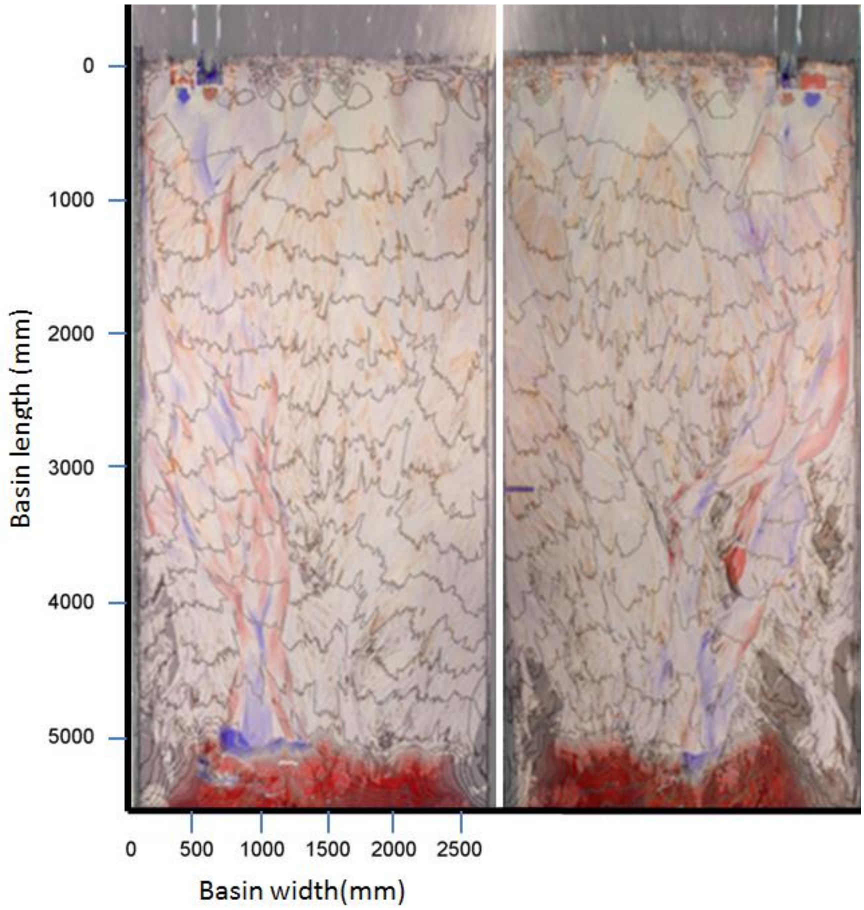

Figure 9: EXP2 Aggradation of B1 and B2, respectively at R204

In EXP2, B2 prograded further into the deep basin compared to B1. This suggests that gradual subsidence has an impact on the total aggradation distance of the system (Fig.9). The constant discharge in B1 and B2 is analogue to general sequence-stratigraphic models that are only affected by relative sea level. Forced regression is observed during sea-level fall (SLF) (R045-084, R105-144, R165-204) and transgression during rapid sea-level rise (SLR) (R035-44, R085-104, R145-164, R205-214) (Fig.6).

Experimental strata

Channel-belt morphology was characterized using the average down-system slope which was calculated at 4 different transect locations (0.5m, 1.0m, 2.0m and 2.2m from the source)(Fig. 10)

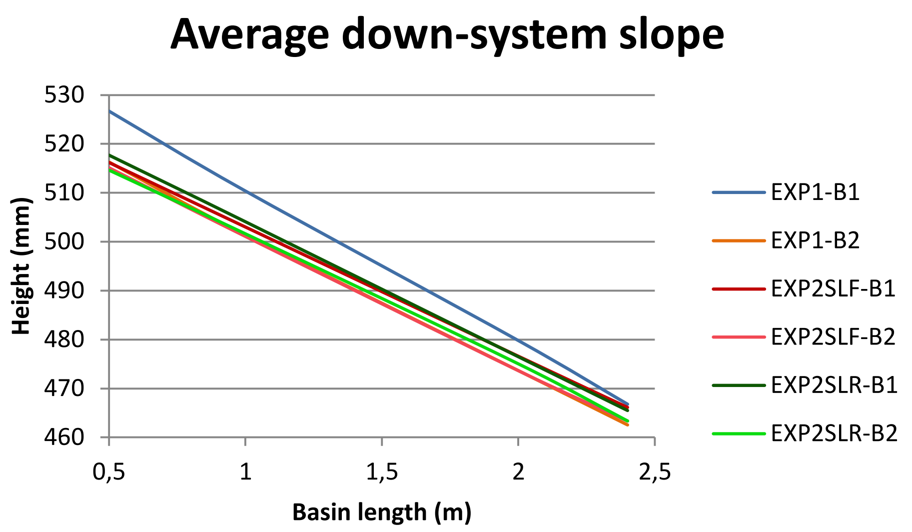

Figure 10: The average down-system slope of EXP1 and EXP2

EXP1-B1 has the steepest slope of 0.0627. EXP1-B2 has a slightly higher slope than EXP2 however there was no major difference in the slope across the basin as all slopes ranged from 0.0527 to 0.0563 (EXP2SLF-B1 to EXP1B2 respectively). Nevertheless, towards the centre of the basin, there was a higher accumulation of deposits during SLR compared to SLF.

SLF and SLR-B1 have a slightly higher topography near the sink compared to B2. This could be due to the slowly subsiding basin in B1.

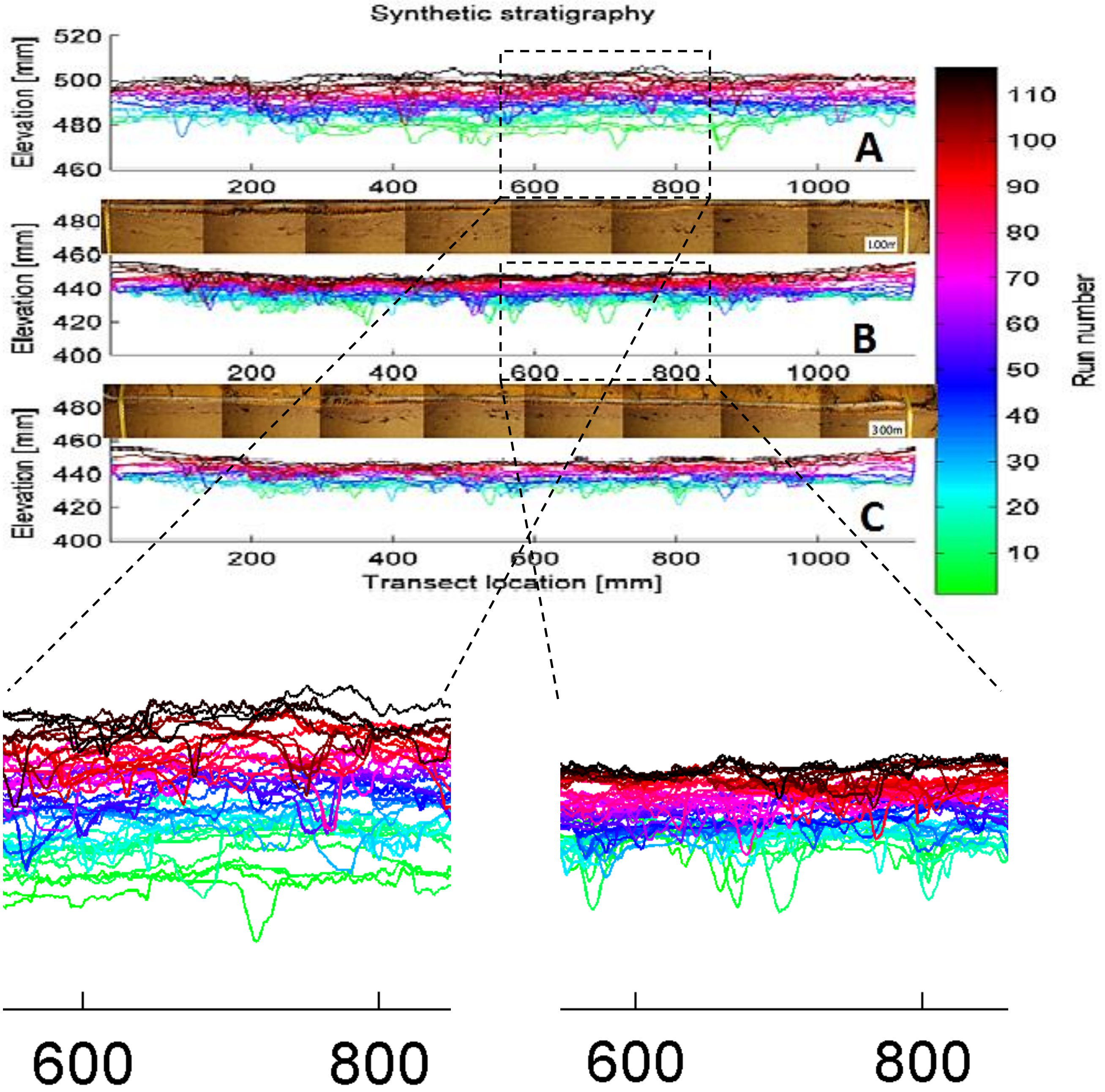

Figure 11: Synthetic stratigraphic panels of final deposition architecture at two measurement transects of EXP1B2 at 1m and 3m (A,B) with their respective lacquerpeel image. The final deposit of B was recreated using every three deposit measurements to lighten the panel, and hightlight so channel areas (C).

At the end of the experiment, the basin was drained and dried. The experimental deposits were vertically sectioned at three laser transects in order to observe the final deposit stratigraphy. Utilising the physical and synthetic stratigraphy (Fig.11) at two measurement transects of the control experiment (EXP1-B2), there is a distinct decrease in density of preserved channel-form bodies away from the source as well as a decrease in the width and depth of preserved channels. Those channel bodies are more linear and appear to be more densely stacked compared to further upstream. The overall width of the aggraded fluvial system is much less at 3.0m from the source compared to 1.0m (Fig.11).

Next, the average wetted fraction, W_f, was estimated by using the dataset from the overhead images of the active transport system. W_f is equal to the total wetted width of the transport system divided by the total basin width (Straub and Wand, 2013) and is used as a proxy for channel width as the high width-to-depth ratio of much of the experimental flows makes directly measuring channel width difficult. The average wetted fraction was measured at transect intervals of 60 cm along the fluvial system of B1 and B2 for both experiments. The measurements started at 0.8m from the source as the dye from the discharged water left some purplish/blue marks on the sand of the fluvial system, mostly dominant in the area near the inlet. W_f was calculated using Matlab. Wet regions were separated from dry regions along the top-set, firstly, by converting the RGB colormap to HSV colormap and, secondly, by defining limits to the hue image and the value image (Fig.12). Using the binary images, the fraction of cross-basin length inundated with water for each image was used to calculate W_f. The average of all W_f for all pictures at the same transect was averaged and plotted against the basin length (Fig.12-13).

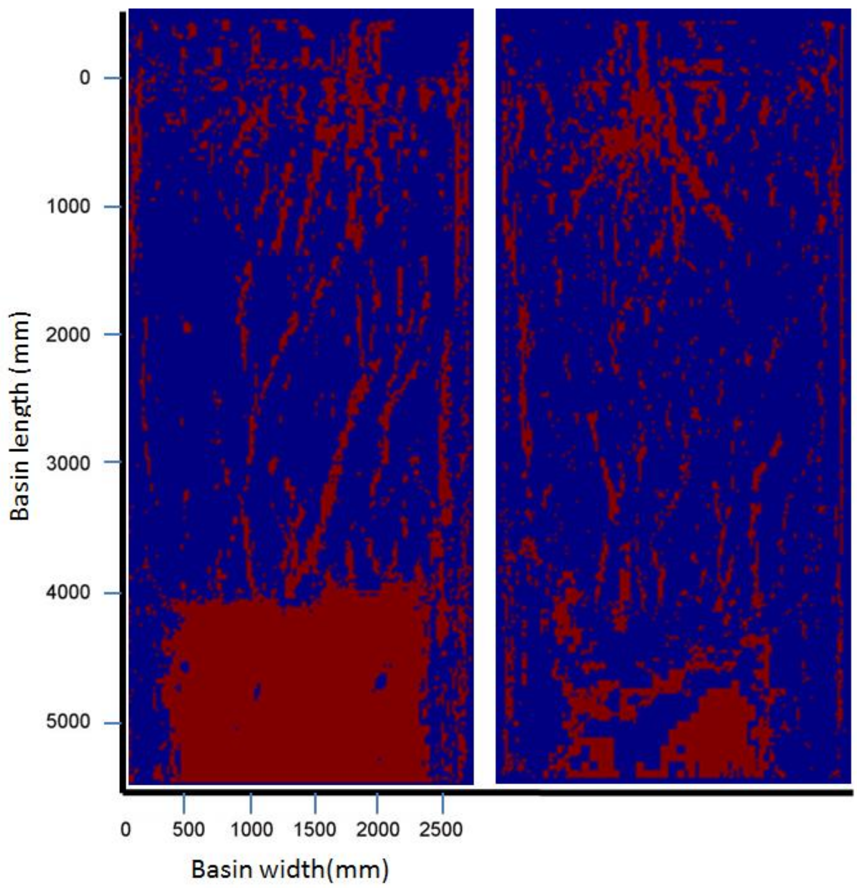

Figure 12: Example of how the picture was changed to binary settings (The red represents the summed flow paths for one run and has a value of 1, the blue is the represents the background and has a value of 0)(EXP1-B1 and B2, respectively of R069)

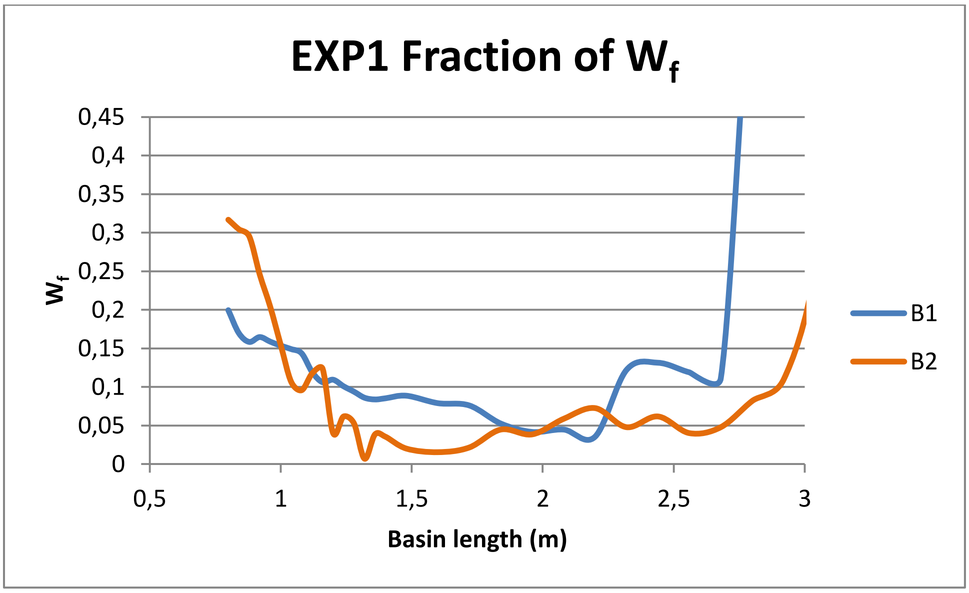

Figure 13: Change in wetted area against basin length

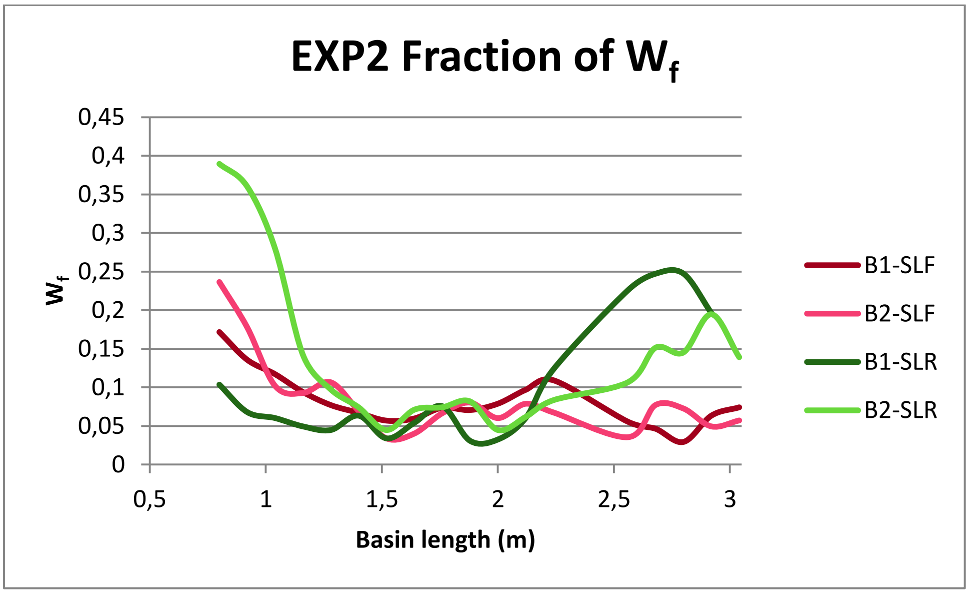

Figure 14: Change in wetted area against basin length

In EXP1, B1 (sand), the wetted fraction experiences a slow but gradual decreases from source to sink, becoming less than the wetted fraction in B2 (walnut-sand mixture) at approximately 2m from the source. Although B2 experiences a very rapid decrease in its wetted fraction upstream, it increases again at approximately 2.0m from the source. As the channel nears the coastline, there is an increase in the wetted fraction for both B1 and B2, suggesting that the channel is levelled with the baseline. In EXP2, both during SLF and SLR, there is a decrease in the wetted fraction around 1.5m from the source, before increasing again from 2.0m.

Another difference that became apparent between EXP1 and EXP2 is the amount of deposition from source to sink. In EXP1, there is an apparent decrease in deposition from source to sink. This is clearly visible in figure 15, as the deposition-erosion models show decrease in the amount of deposition in EXP1 from source to sink, however, in EXP2, deposition is constant across the fluvial system. Sea-level changes appear to have a positive correlation with sediment transport throughout the fluvial system (Fig.15).

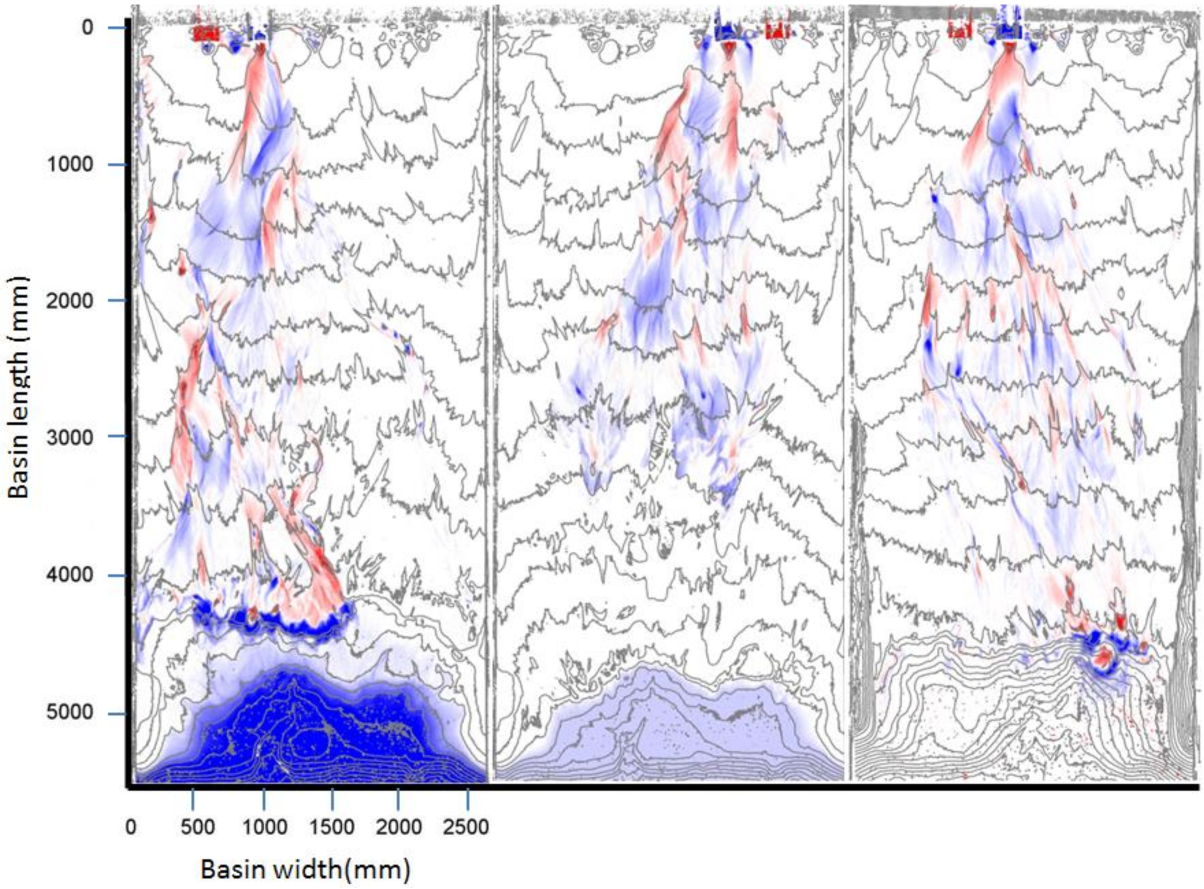

Figure 15: Difference in deposition-erosion between sea-level change (SLF and SLR respectively) and no sea-level change (EXP2B1-R130,102 and EXP1B2-R153, respectively)

Strength and time scales of compensation

Through the use of topographic datasets, σ_{ss} was calculate from 0.4m from the source and at every 4cm topographic transect along the fluvial system and for every possible pair-wise combination of topographic surveys, in order to define the decay of σ_{ss} over an interval window of 1-115runs (1- 3450 minutes) for EXP1 and 1-179 (1-5370 minutes) for EXP2. To optimise the results and obtain a smoother curve, the average of 15 transects lines was used (Appendix 1). The method to measure the degree of compensation in the system was slightly altered from the one brought forward by Straub et al. (2009). Noticing that long term sedimentation varies according to the point in space, it was important to take every time interval into account at every time step so as to obtain the most accurate results possible (Appendix 2). Instead, *r^(x)* represented the local long term sedimentation rate at the next local sedimentation point, thus taking the exact sedimentation deposition pattern into account.

Before calculating σ_{ss}, the effect of the inlet position on deposition was analysed. For that, the number 1 was given to the inlet when it was used, number 2 when it was used a second time and so on. This created a 115x12 matrix (number of runs x number of possible inlet positions) with the following end-topography:

12	7	9	4	17	8	7	14	9	8	10	13

The compensation index was calculated using solely the inlet position to create a synthetic model. κ was found to be random at all time intervals with no κ_n. The inlets show pure random behavior and what to expect if the system did not have any controlling factors (Fig.16).

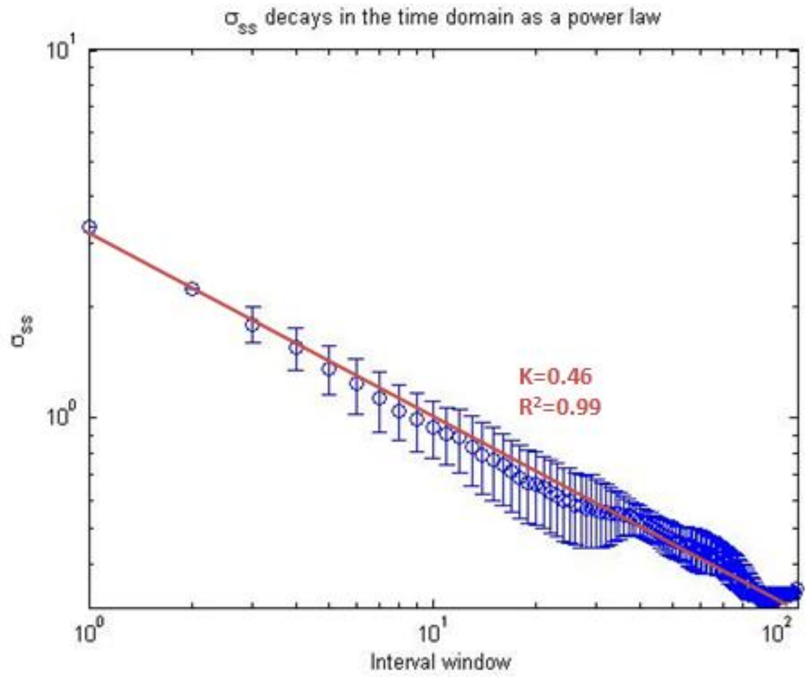

Figure 16: Compensation index based solely on inlet position

The variability in sedimentation was then investigated for EXP1 and EXP2.

The decay of σ_{ss} was plotted as a function of time and found that for all data sets, the magnitude of κ over short time scale ($< \kappa_n$) is less than the magnitude of κ measured over long time scales ($>\kappa_n$) (Fig.21 -23). For all data sets of EXP1, κ_1 (below κ_n) is between 0.3 – 0.65. indicating that over these time scales, space is filled somewhere between persistant in deposition trend (anti-compensational) and compensationally. However, at time scales above κ_n, the basins show a gradual increase from compensational to purely compensational filling.

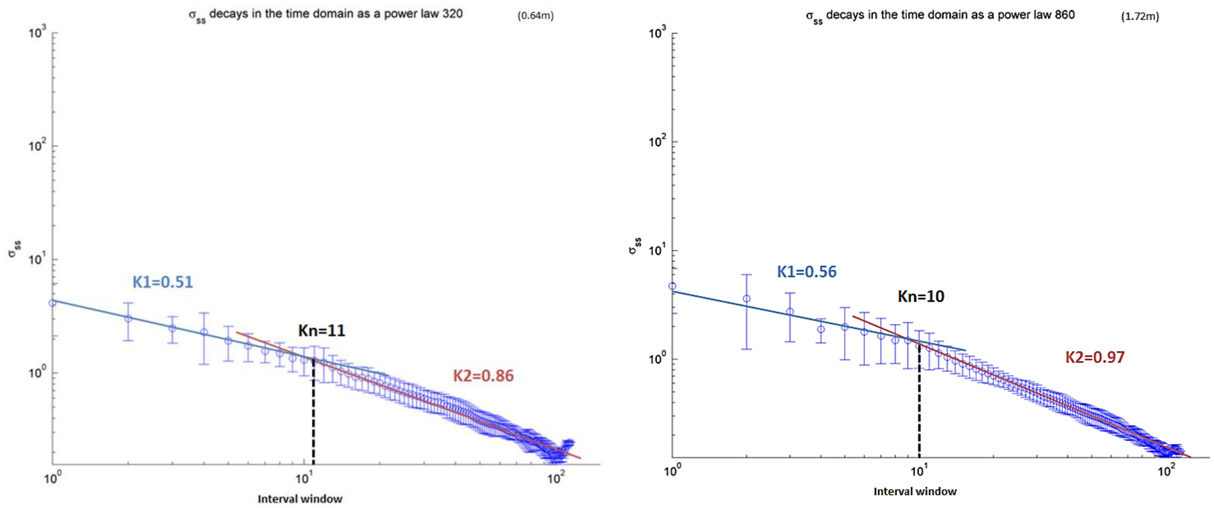

Figure 17: EXP1 Decay of σ_{ss} as function of interval window at different locations along the fluvial system for B1. Error bars represent geometric standard deviation.

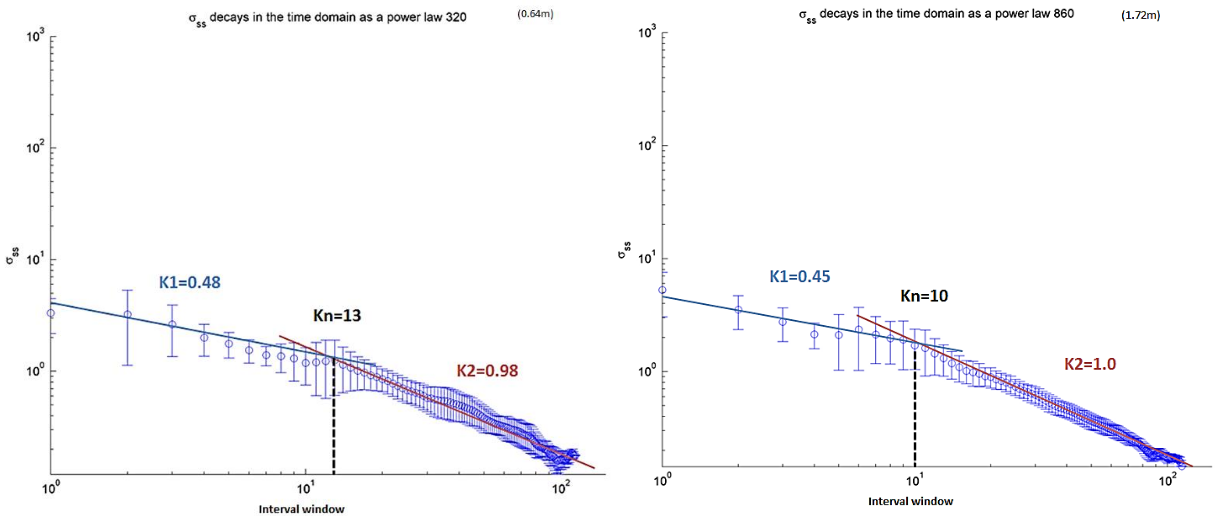

Figure 18: EXP1 Decay of σ_{ss} as function of interval window at different locations along the fluvial system for B2. Error bars represent geometric standard deviation.

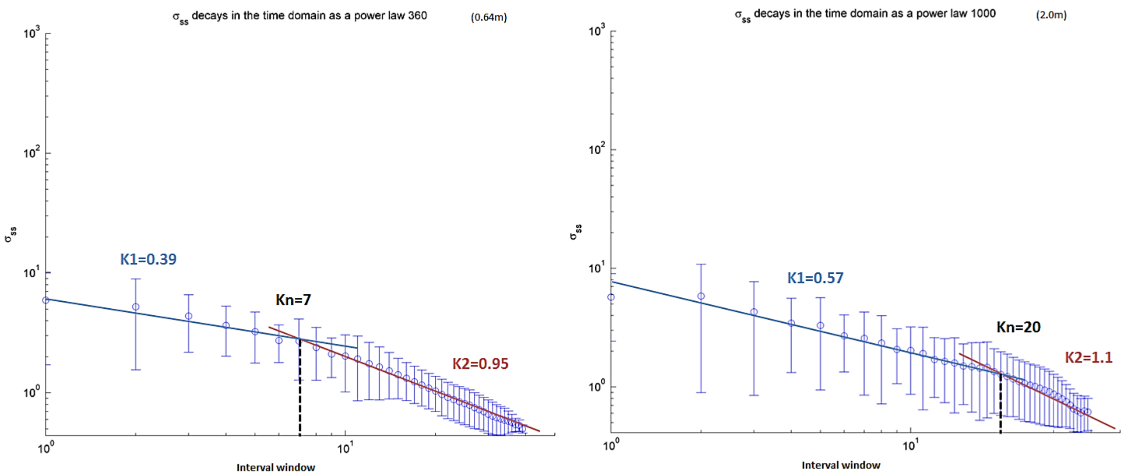

Figure 19: EXP2-SLF Decay of σ_{ss} as function of interval window at different locations along the fluvial system for B1. Error bars represent geometric standard deviation.

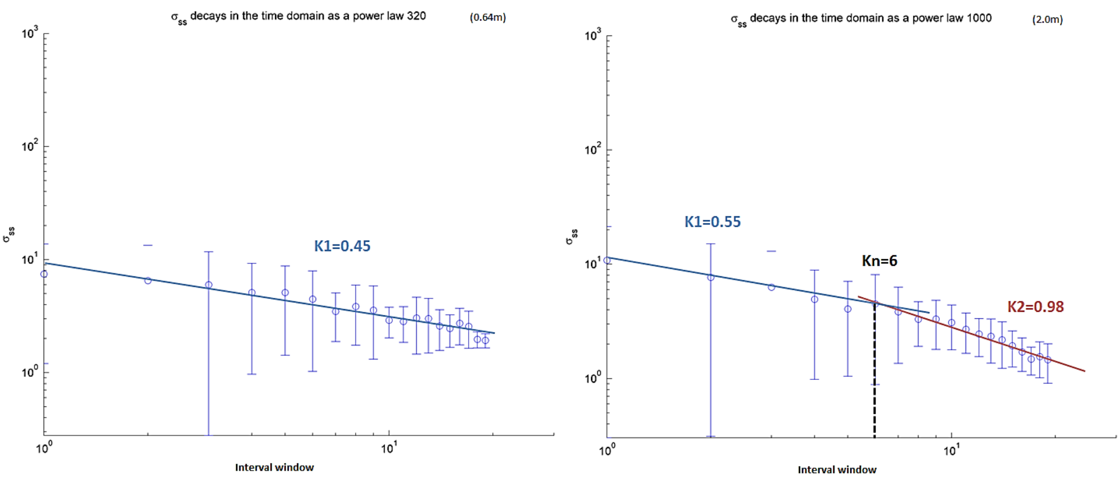

Figure 20: EXP2-SLR Decay of σ_{ss} as function of interval window at different locations along the fluvial system for B2. Error bars represent geometric standard deviation.

Another important observation is the time scale at which the experiments become fully compensational. EXP1 and EXP2 show differing patterns in κ_n. EXP1, B1(sand) shows that, in the medial part of the basin (between 1m and 1.7m from the source) there is a sudden decrease in the time scale at which it becomes fully compensational (from 5.5hrs to 2.5hrs). The time scale increases again as the systems gets closer to the coastline. B2 shows a gradual decrease in κ_n from source to sink (from 6.5hrs to 4hrs) (Fig.21).

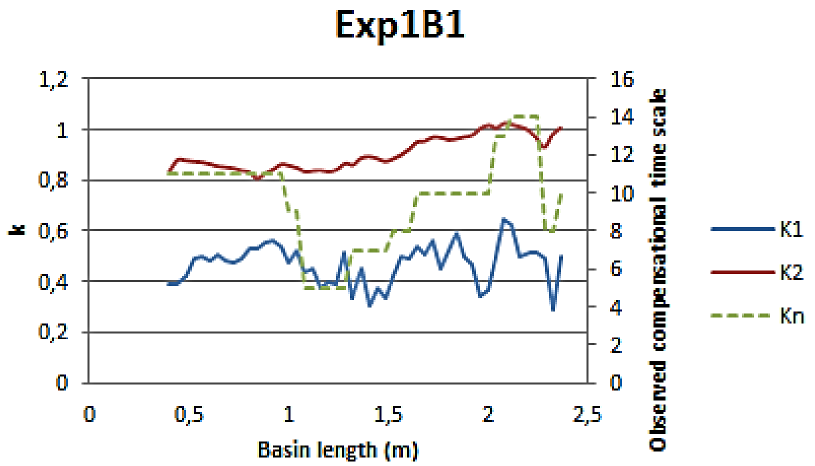

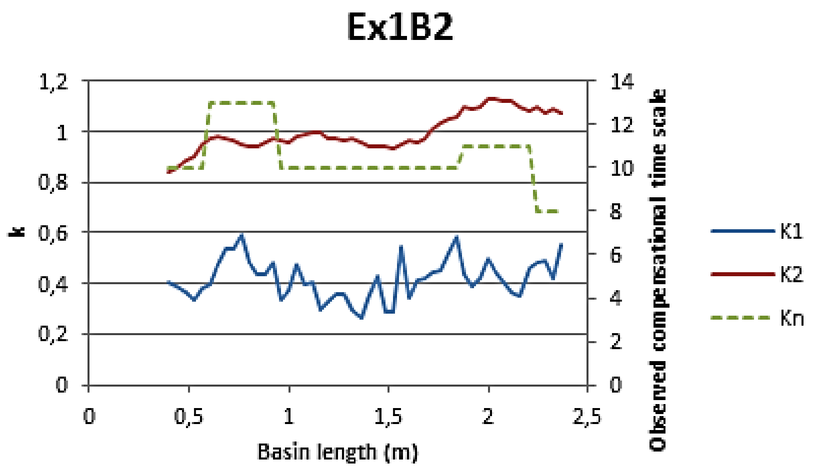

Figure 21: Changes in κ_1, κ_2 and κ_n along the fluvial system (EXP1)

κ_1 in both B1 (purely sand) and B2 (sand-walnut) remains random across the fluvial system. As the inlet in both experiments were randomly positioned, the results in figure 21 show that this randomness remains the same from source to sink. κ_2 also shows an increase from compensational to fully compensational in both basins, however that change is even more prominent in B1. The main difference between both basins is the time scale at which B1 and B2 become fully compensational. Both basins show an overall decrease in κ_n, but B1 has very short time scales towards the centre of the basin.

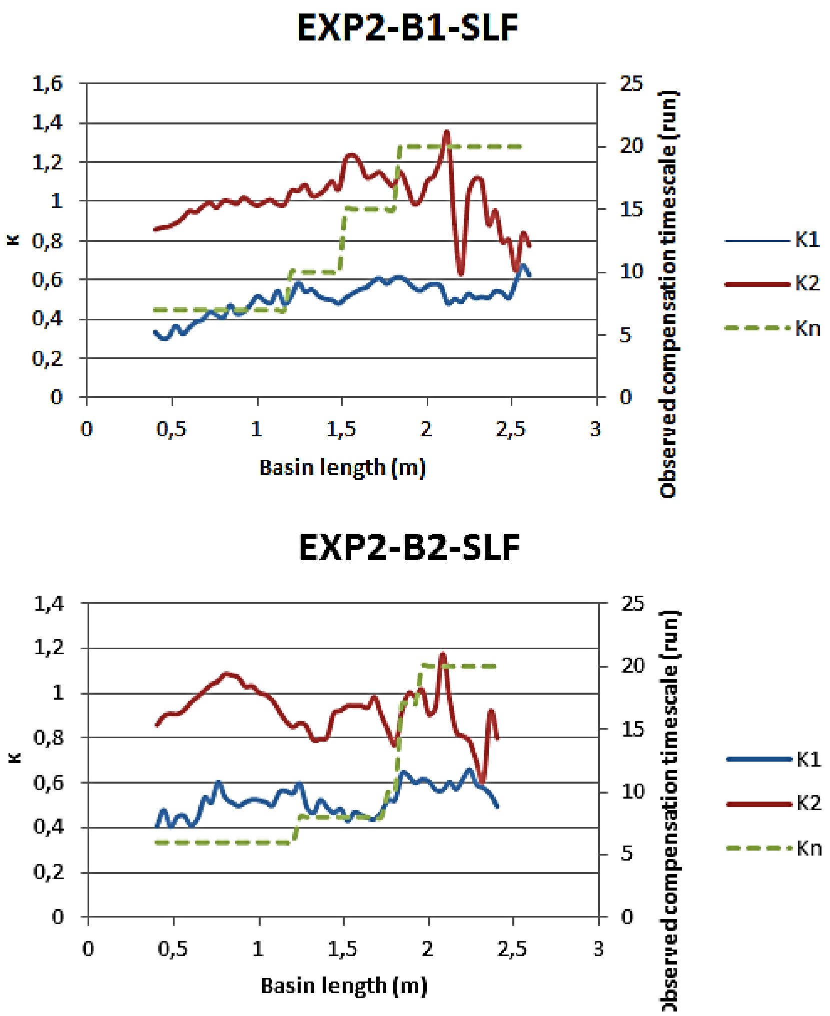

Figure 22: Changes in κ_1, κ_2 and κ_n along the fluvial system (EXP2-SLF)

During sea-level fall (Fig.22) , κ_1 is random but gradually becomes more compensational from source to sink. There is an overall increase in the time scale at which the system becomes fully compensated. However, all data sets of EXP2-SLF suggest that, at approximately 1.2m from the source, the system experiences changes which leads to an increase in κ_n over the length of the basin. The time scales for both B1 and B2 start at 2.5hrs near the source (remember that each run lasts 30minutes).

For the data sets representing sea-level fall in EXP2, κ_1 is between 0.30 and 0.67, indicating that over these time scales, space as filled somewhere between anti-compensationally and randomly. κ_2 in both basins is fully compensational.

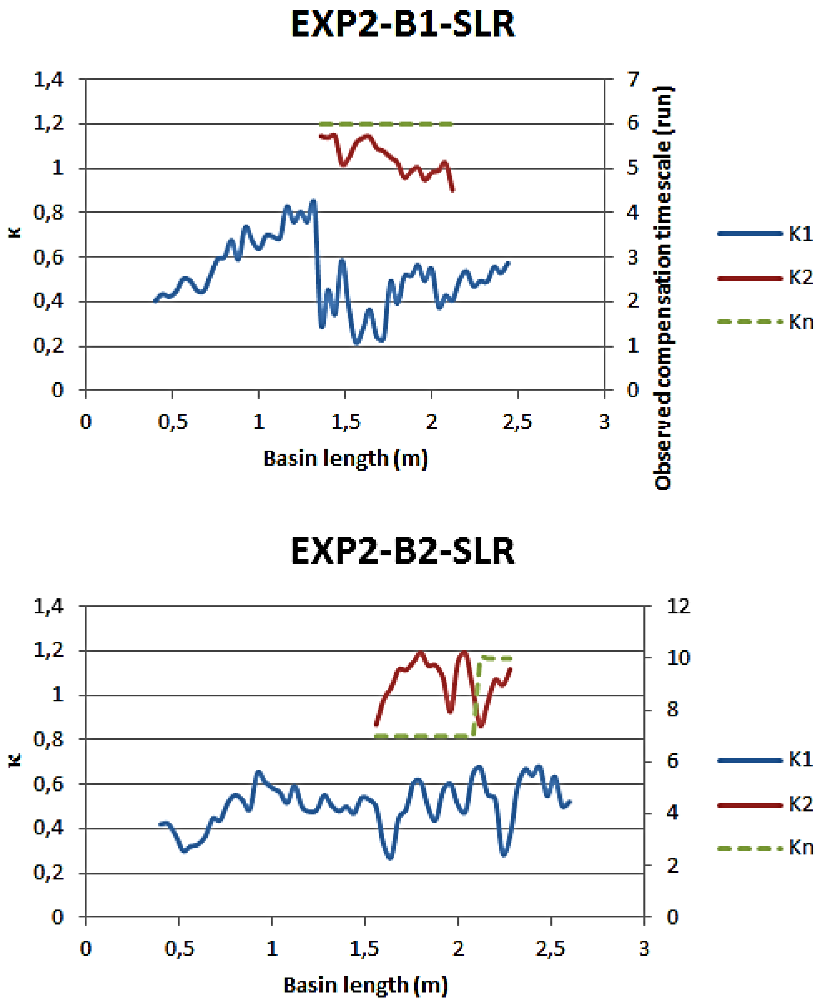

Figure 23: Changes in κ_1, κ_2 and κ_n along the fluvial system (EXP2-SLR)

During sea-level rise (Fig.23), κ_1 is between 0.21 and 0.81, suggesting that the space was filled somewhere between anti-compensationally and compensationally. However, the results obtained during SLR do not inlude κ_n for the entire fluvial system as it was not reached as there was a total of 20 runs (10hrs) with SLR. However, κ_n does seem to reach full compensation between approximately 1.4m to 2.3m from the source. If there had been a longer SLR, maybe there would have been more information concerning the time scales at which the proximal area to the source reaches full compensation. But, these results show that the medial part of the basin during SLR, reaches compensation prior to the proximal and distal parts. Unfortunately, the results obtained during SLR, contain information over 20runs (10hrs) so this could explain why full compensation is not obtained.

Finally the coefficient of variation was applied to EXP1-B1, as Straub and Pyles (2012) suggested that it would be a good proxy for σ_{ss} when the basin in undergoing uniform and constant subsidence and rates are unknown. Similar to the equation of Straub et al. (2009), CV (coefficient of variation) uses the local deposit thickness between stratigraphic surfaces instead of using the rate. From the results in figure 24, CV does fit with σ_{ss}, κ_{cv} is more difficultly defined than κ especially as we move away from the source where the deposit thickness becomes less.

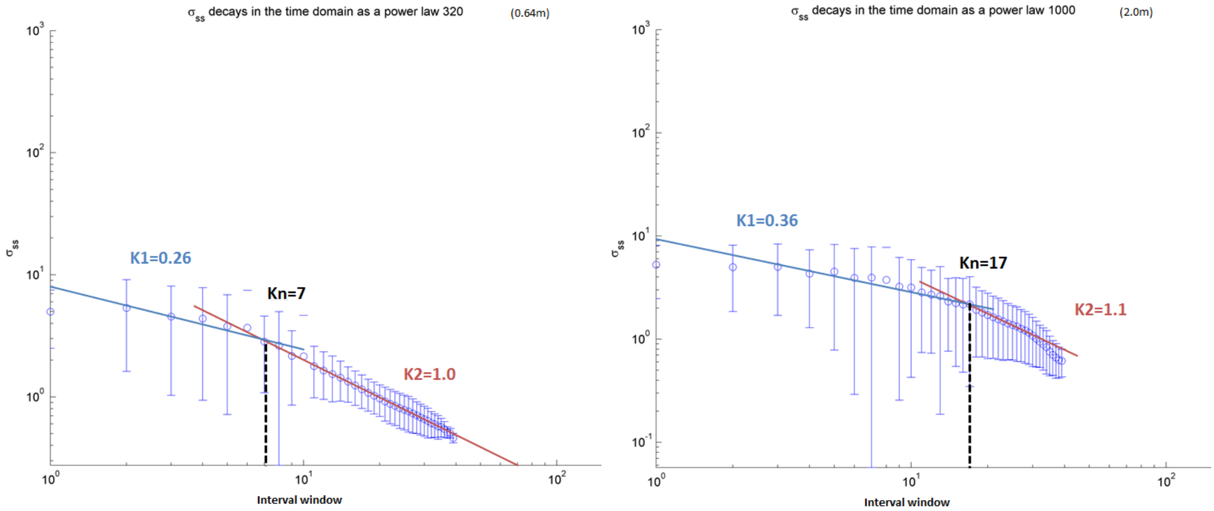

Figure 24: κ_{cv} of EXP2-SLF-B1 at 0.64 and 2.0m from the source, respectively

Values of κ_1 and κ_2 are relatively similar to the method used in this paper, however, κ_n is more difficultly to define.

5. Discussion

The main goal of this study is to characterize how changes in external controls affect the stacking pattern of channel-belts. For that, the effect of the sediment composition, sea level change and subsidence were studied.

Influence of walnut-sand mixture and pure sand on the long time scale autogenic processes

The addition of walnut-shell and saline water to EXP1-B2 is a simple bimodal mixture that displays strong and readily measurable hydraulic sorting by processes analogous to those that produce size sorting in nature. Furthermore, the use of saline water could have a different effect on channel formations as it is denser than fresh water. For those reason, B2 served as the control experiment.

The aggradation in EXP1-B1 was higher than that of B2. Walnut-shell has a lower density than sand grains and can therefore travel further down the system than a sand grain under the same condition. Since walnut-shell represented 33% of the total mixture, it is understandable that the slope of the basin with walnut-sand mixture will be lower than the same basin consisting of only sand grains. The difference in topography between the two basins will result in B2 prograding further into the deep basin compared with B1 (Fig.7). The strength of compensation, and thus stratigraphic organization is near identical for both basins, with B1 stacking slightly more randomly than B2 before κ_n (Fig.21), thus suggesting that the random behaviour of the inlets play a role in determining the autogenic processes. Those results suggest that B1 and B2 fill space in a statistically similar fashion, but over different time scales. Concerning this last point, it is worth to note that, along the fluvial system, the time scale of compensation was shorter for B1 than B2. The short time scale at the centre of B1 could indicate that, as only sand was present in the system, the time needed for channels to visit every spot in the medial part of the basin several times, was less than that of B2 which had further travelling elements and more channelized flow. This is observable when looking at the W_f (Fig.13) which is much higher in the medial part (1.3m-1.7m from the source) of B1(sand) compared to B2. This would have influenced the overall deposition pattern and thus explaining why there is a lower time scale at which full compensation is reached in B1. The range of scales at which autogenic processes operate was therefore shorter in B1 than B2 in the medial area but both basins experienced an overall decrease in κ_n.

Influence of sea-level changes

As mentioned in the theoretical analysis part of this paper (section 2), external controls such as glacio-eustatic sea-level variation and lateral variations in the depth of the receiving basin are known to have a strong influence on the areas of accommodation and deposition (e.g. Posamentier et al*.,* 1988), therefore strongly affecting the location of channels, as well as their stacking pattern.

By inducing sea-level changes, the behaviour of basin filling sedimentation patterns was determined during sea-level fall and sea-level rise. The strength of compensation was compared between both basins, by looking at sea-level rise and sea-level fall individually. B1 and B2 had similar κ_1 values as well as κ_2 values.

An explanation for the changes in κ_n along the fluvial system could be due to the channel-belt morphology. Nearer the source, the flow depends on the inlet position, however, as is move downstream it becomes less dependent on the inlet position and more on the topography of the basin. During sea-level rise (SLR), the morphology of the channel-belt alters. This is deduced from the W_f of SLR compared to SLF (Fig.14) when nearing the sink. The area near the inlet reaches its compensation time scale rapidly whereas, in the medial part, the basin is adapting to transgression which increase the compensational time scale . As sea-level falls (SLF), the channel-belt constantly migrates with respect to the inlet position and has a longer way to compensate to reach the sink. The channel-belt morphology was shown to be narrower than that of SLR (Fig.14) which could be explained by more channelized migration from the medial section onwards, as the channel belt needs to travel further with sea-level falls. This results in the system needing more time to become fully compensational as less area is repeatedly visited by the channel-belt.

As stated by Straub and Pyles (2012), some sedimentary systems tend to move across and fill basins randomly and chaotically, while others deposit in a structured, even manner. For example, a channel forming during sea-level rise can migrate across a basin to fill it more evenly than more cohesive laterally-restricted deltaic system (i.e. Sea-level fall).

Powell et al. (2012) concluded that an increase in sediment supply in a deltaic system will primarily decrease the autogenic time scale. However, the increase in sediment supply does not proportionally reduce the autogenic time scale because the increase in sediment supply affects the morphology of the fluvial system by developing a relatively larger fluvial buffer system to be filled during times of sediment storage (Powel et al. 2012). From the results obtained in this study, Powell et al. (2012)'s statement appears to be partially true in the case of a system with no external forcing. The increase in deposition during sea-level change along the fluvial system probably increased the autogenic time scale in EXP2 during SLF as κ_1 changes from random to compensational stacking from source to sink.

Influence of subsidence

The deep basin area of B1 was gradually subsiding. At the start of the EXP2, the deep basin was hardly subsided, and after every 10 runs, the basin was subsided a little more. Subsidence does not appear to have much impact on κ_1 and κ_n. κ_1 in B1 is more fully compensated than κ_1 in B2. This could be explained by the slope of the deep basin. Due to the steeper slope during SLF (0.0546) compared to SLR (0.0538) in B2, the sediments deposited along the top-set and at the bottom of the deep basin resulting in limited progradation (Fig.10). In B1, the deep basin was much more shallow at the beginning of the experiment, which led the sediments deposited during SLF to prograde along a shallower slope (0.0527 compared to 0.0546 in B1 and B2 of SLF, respectively)much further into the deep basin (Fig.27).

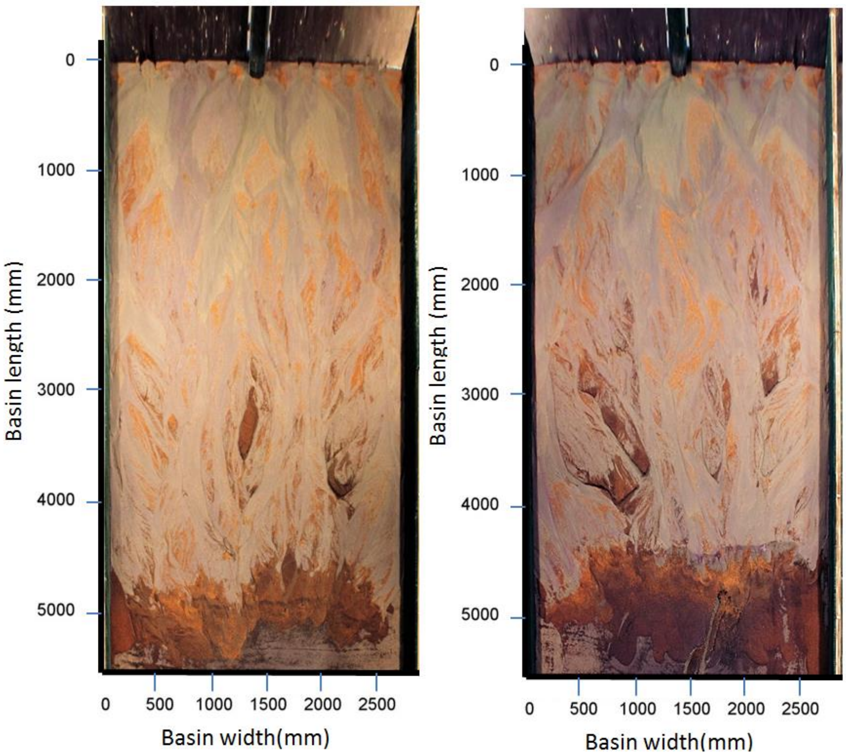

Figure 27: EXP2 Empty basins of B1 and B2 respectively at the end of R079

Changes from source to sink

In the experiments, sea-level change influences the behaviour of basin filling patterns.

In the region near the source, there are interconnected stacked channel bodies (Fig. 12) which form as a result of their proximity to the inlet area and higher topography. Towards the centre area of the experiments, there is an increase of the submerged area and a gradual decrease in the slope difference suggesting a more widespread preference of the channel-belt (Fig.13-14). Finally, the region closest to the sink shows an increase in the wetted area during sea-level rise and decreases during sea-level fall. This affects the morphology of the channel-belt at distal areas with more channelized elements during SLF as the channels had less energy and sediments to cover the top-set and instead followed the topographic low. The total distance travelled during SLR was less, they show a more spread out morphology closer to the sink (Fig.15). These source to sink changes in stratigraphic architecture are associated with a decrease in organization of basin filling patterns, as characterized by a decrease in κ_n during constant sediment discharge and no sea-level changes .This trend could be related to the observed decrease in the variance of deposition rate from source to sink (Fig.14). During SLF. W_f suggest more channelized elements which could explain the increase in κ_n from source to sink.

Ganti et al. (2011), show that all the truncation scales on their random variables studied are set either by the channel depth-space statistics or the characteristic avulsion time scales of the channels (time statistics), indicating that channel depths act as a first-order control on the structure of surface dynamics and preserved stratigraphy in depositional systems. Straub and Wang (2013) see an increase in channel depth when the ratio of water discharge is higher than that of sediment discharge, thus resulting in higher κ_1 values compared to when the ratio between water and sediment discharge is constant. In EXP2, SLR led to changes in the area where more sediments were deposited. These sediments were then eroded away during SLF which resulted in an increase in mobile sediments compared with EXP1 (Fig.15). This increase could explain the difference in κ_1 values between EXP1 and EXP2. In EXP1, there is a decreasing trend of κ_n from source to sink which could be the result of the decrease in channel depth with transport distance in EXP1 as the long term sedimentation rate was spatially constant in the first experiment. Even though there were no experiments to show that channel depth decrease from source to sink, figure 11 shows a decrease in density of preserved channel-form bodies from source to sink as well as a decrease in the width and depth of preserved channels.

Furthermore, there is a decrease in the amount of deposition in the medial part of the basin during EXP1, compared to higher sediment deposits during EXP2-SLF (Fig.15). This suggest that, even though the channel depth was not calculated, it would be reasonable to assume that, in EXP1, channel depth decrease from source to sink resulting in a proportional decrease in κ_n compared to an increase in channel depth from sink to source which also show a respective increase in κ_n. Changes in sea-level affect deposition, thus affecting channel depth, which could be the explanation for the increase in κ_n from source to sink (Fig.22).

For field-scale systems with near spatially uniform deposition rates, results from EXP1 suggest that preservation of paleo-environmental (allogenic) signals is optimized at distal settings where the range of time scales over which autogenic processes operate is minimized. However, in systems with spatially variable sea-level changes, there is a source to sink increase in κ_n which suggests that the preservation of paleo-environmental signals would be optimized in proximal settings, away from areas influenced by sea-level changes.

Time scale compensation in field scale systems

Wang et al. (2011) estimated κ_n for the Lower Mississippi Delta region using known depths of the Mississippi River and long term sedimentation rated from biostratigraphy information and found that κ_n was 115k.y, a value ~100 times greater than the ~1300 yr re-occurrence interval for larger avulsions of the Lower Mississippi River (Wang et al.2011). Straub and Wang (2013) compiled a larger data set of κ_n estimates for field scales basins using published data on river depth and long term sedimentation rates and included thirteen modern delta systems (Fig.28).

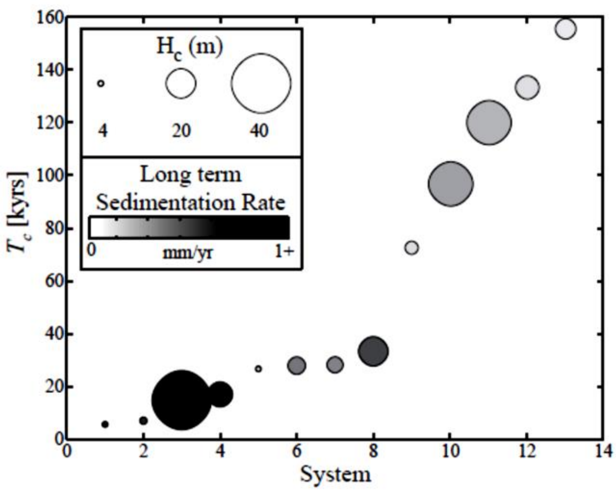

Figure 28: Tc (κn) estimates for compilation of thirteen modern delta systems uing published data on channel depth and long term deposition rate (measurement interval in excess of 100kyrs). Sizeof circle scales with depth of a system's channels while grayscale value of circle fill scales with the long-term sedimentation rate of a basin (Straub and Wang 2013)

For the thirteen systems, they estimated κ_n values between 5.6 and 156kyrs. The duration of many of these systems overlap or is longer than the period of the Earth's eccentricity (100,000yrs), inclination (70,000yrs), obliquity (41,000yrs), axial precession (26,000yrs), or apsidal precession (21,000yrs) cycles. These Milankovitch cycles impact the amount of solar radiation entering the atmosphere, specifically the amount of solar radiation entering the atmosphe4re during summer months at high latitudes, thus strongly influencing the size of high latitude glaciers and thus, having a direct impact on global eustasy, a commonly discussed allogenic forcing (Straub and Wang, 2013). These examples highlight the large amount of time necessary for autogenic surface-process dynamics to average out in the stratigraphic record, thus supporting the results found in this paper.

Importance of channel stacking understanding (3D Seismic)

With the use of the ever advancing technology, industry-grade 3D seismic survey from a fluvial system is utilised by Straub et al. (2009) to measure the decay of σ_{ss} or CV in a terrestrial field-scale basin. The findings are used to predict the type of system: valley, tectonic zone, sea proximity, channel or unchannelized dominated area.

According to Wang et al. (2011), industry-grade seismic data resolution is such that σ_{ss} cannot be measured for deposits with a mean thickness of < ~20m (magnitude of many channel depths). Instead, outcrop-based studies are used, in which the stratigraphic architecture can be mapped above and below the scale of individual channel bodies. Straub et al. (2009) applied their findings directly to geostatistical reservoir models that use compensational stacking routines to fill model space.

Previous models, such as the stochastic surface based model of turbidite lobes, developed by Pyrcz et al. (2005), used algorithms to place architectural elements within a model domain which is in perfect compensational stacking of turbidite lobes (κ = 1). However, this is suggested to represent only the end member scenario. It is therefore important to obtain a better understanding of controls on the compensation index κ through the use of various simulation scenarios.

Straub and Pyles (2012), argue that these models can be used by the oil and gas industry for:

- Making production forecasts through fluid-flow simulations
- Improving one's ability to predict static connectivity in deep water reservoir or fluvial system reservoir.

6. Conclusion

Through physical experiments, the influence of sediment mixture, sea-level change and subsidence on the strength and time scales of autogenic processes in alluvial basins was examined. The main results are summarized as follows:

1. Sediment texture influences the organization in basin filling along a source to sink paths. Low density sediments will favour formation of channel paths whereas high density sediments will deposit over a wider range. We found that the systems with different sediment mixture will fill basins in a statistically similar fashion, but over slightly differing time scales.
2. Sea-level change leads the increase in compensational stacking from source to sink with a corresponding increase in the time scale at which the basin becomes fully compensational
3. Subsidence influences the progradation of the top-set, with no significant impact on the organization of the channels and the time scale at which they become fully compensated.

7. References

Allen, J. (1979) Studies in fluviatile sedimentation; an exploratory quantitative model for the architecture of avulsion-controlled alluvial sites. Sedimentary Geology, 21, 129–147.

Blum, M., Martin, J., Milliken, K. and Garvin, M. (2013) Paleovalley systems: Insights from Quaternary analogs and experiments. Earth-Science Reviews, 116, 128-169.

Blum, M. and Törnqvist, T. (2000) Fluvial response to climate and sea-level change: a review and look forward. Sedimentology, 47, 2-48.

Edmond, D.A., and Slingerland, R.L. (2010) Significant effect of sediment cohesion on delta morphology. Nat Geosci, 3(2), 105-109.

Eisele, G., Ricken, W., and Seilacher, A. (1991) Cycles and events in stratigraphy. Berlin, Springer-Verlag, 1-140.

Hajek, E., Heller, P. and Sheets, B. (2010) Significance of channel-belt clustering in alluvial basins. Geology, 38, 535-538.

Heijst van, M. and Postma, G. (2001) Fluvial response to sea-level changes: a quantitative analogue, experimental approach. Basin Research, 13, 269-292.

Hoyal, D. C.J.D., and Sheets, B.A. (2009) Morphodynamic evolution of experimental cohesive deltas. Journal of Geophysical Research, Earth Surface, 114.

Jerolmack, D.J., and Paola, C. (2007) Complexity in a cellular model of river avulsion. Geomorphology, 91, 259-270.

Jerolmack, D.J., and Paola, C. (2010) Shredding of environmental signals by sediment transport. Geophysical Research Letters, 37.

Leeder, M. (1978). A quantitative stratigraphic model for alluvium, with special reference to channel deposit density and interconnectedness. Memoir - Canadian Society of Petroleum Geologists 5, 587-596.

Lyons, W.J. (2004) Quantifying channelized submarine depositional systems from bed to basin scale [unpublished Ph.D. thesis]. Woods Hole Oceanographic Institution and Massachusetts Institute of Technology, Woods Hole, Massachusetts, 1-252.

Macdonald, H.A., Peakall, J., Wignall, P.B., and Best, J. (2011) Sedimentation in deep-sea lobe-elements: implications for the origin of thickening-upward sequences. Geological Society of London, Journal, 168, 319-331.

Mackin, J.H. (1948) Concept of the graded river. Geological Society of American Bulletin, 59, 463-512.

Morhig, D., Heller, P.L., Paola, C., and Lyons, W.L. (2000) Interpreting avulsions process from ancient alluvial sequences: Guadalope-Matarranya (northern Spain) and Wasatch Formation (western Colorado). Geological Society of America Bulletin, 112, 1787-1803.

Muto, T., Steel, R. and Swenson, J. (2007) Autostratigraphy: a framework norm for genetic stratigraphy. Journal of Sedimentary Research, 77, 2-12.

Mutti E., and Normark, W.R. (1987) Comparing examples of modern and ancient turbidite systems: problems and concepts. Marine Clastic Sedimentology; Concepts and Case Studies: London, Graham and Troman, 1-38.

Mutti, E., and Sonnino, M. (1981) Compensational cycles: a diagnosis feature of turbidite sandstone lobes: International Association of Sedimentologists, Second European Regional Meeting, 120-123.

Paola, C., Hellert, P., Angevinet, C. (1992) The large-scale dynamics of grain-size variation in alluvial basins, 1: theory. Basin Research, 4, 73-90.

Paola, C., Straub, K., Mohrig, D., Reinhardt, L. (2009) The 'unreasonable effectiveness" of stratigraphic and geomorphic experiments. Earth-Science Reviews, 97, 1-43.

Posamentier, H. and Vail, P. (1988) Eustatic controls on clastic deposition II – sequence and system track models. Sea-Level Changes: an Integrated Approach, 42, 125-154.

Postma, G., Kleinhans, M.G., Meijer, P. Th. and Eggenhuisen, J.T. (2008) Sediment transport in analogue flume models compared with real-world sedimentary systems: a new look at scaling evolution of sedimentary systems in a flume. Sedimentology, 55, 1541-1557.

Powell, E.J., Kim, W., and Muto, T. (2012) Varying discharge controls on timescales of autogenic storage and release processes in fluvio-deltaic environments: Tank experiments. J Geophys Res-Earth, 117, F02011, doi:10.1029/2011jf002097.
Prelat, A., Covault, J.A., Hodgson, D.M., Fildani, A., and Flint, S.S. (2010) Intrisic controls on the range of volumes, morphologies, and dimensions of submarine lobes. Sedimentary Geology, 232 66-67.
Pyrcz, M.J., Catuneanu, O., and Deutsch, C.V. (2005) Stochastic surface-based modeling of turbidite lobes. American Association of Petroleum Geologists, Bulletin, 89, 177-191.
Ganti, V., Straub, K.M., Foufoula-Georgiou E., Paola, C. (2011) Space-time dynamics of depositional systems: Experimental evidence and theoretical modelling of heavy-tailed statistics. Journal of Geophysical Research, 116, 1-17.
Sheets, B.A., Hickson, T.A. and Paola, C. (2002) Assembling the stratigraphic record: depositional patterns and time-scales in an experimental alluvial basin. Basin Research, 14, 287-301.
Sheets, B.A., Paola, C., and Kelberer, J.M. (2007) Creation and preservation of channel-form sand bodies in an experimental alluvial system. Sedimentary Processes, Environments and Basins, Blackwell Publishing, Oxford, U.K., 555-567.
Slingerland, R.L. (1990) Predictability and chaos in quantitative dynamic stratigraphy, *in* Cross, T.A., ed., Quantitative dynamic stratigraphy. Englewood Cliffs, New Jearsey, Prentice-Hall, 45-53.
Straub, K.M., and Esposito,C.R. (2013) Influence of water and sediment supply on the stratigraphic record of alluvial fans and deltas: Process controls on stratigraphic completeness. Journal of Geophysical Research-Earth Surface, 118, 13, doi:10.1002/jgrf.20061.
Straub, K.M., and Mohrig, D. (2008) Quantifying the morphology and growth of levees in aggrading submarine channels. Journal of GEOPHYSICAL Research, Earth Surface, 113.
Straub, K.M., Paola, C., Mohrig, D., Reinhardt, L. (2009) The 'unreasonable effectiveness' of stratigraphic and geomorphic experiments. Earth Science Reviews, 97, 1-43.
Straub, K.M. and Pyles, D.R. (2012) Quantifying the hierarchical organization of compensation in submarine fans using surface statistics. Journal of Sedimentary Research, 82, 889-898.
Straub, K.M., and Wang, Y., *in press* (2013) Influence of water and sediment supply on the long-term evolution of alluvial fans and deltas: Statistical characterization of basin-filling sedimentation patterns. Jounral of Geophysical Research-Earth Surface, DOI: 10.1002/JGRF.20095.
Vail, P.R. (1987) Seismic stratigraphy interpretation utilizing sequence stratigraphy Part 1 – Seismic stratigraphy interpretation procedure. Atlas of seismic stratigraphy, 27, AAPG studies in geology, edited by WW.Bally, 1-10.
Wang, Y., Straub, K.M. and Hajek, E.A. (2011) Scale-dependent compensational stacking: An estimate of autogenic time scales in channelized sedimentary deposits. Geology, 39, 811-814.
Weimer, P., and Link, M.H. (1991) Seismic facies and sedimentary process of submarine fans of submarine systems. New York, Springer-Verlag, 9-67.

8. Acknowledgments

Firstly, I thank Joris Eggenhuisen for being my supervisor and for giving me the opportunity to do this research at the Eurotank Flume Laboratory at Utrecht University. I am grateful for his great guidance since the start of my research.

Secondly, I thank Jochem Bijkerk for allowing me to participate in his experiments, for giving me continuous guidance and feedback as well as great advice with the MATLAB analysis. His passion on the subject made my time in the lab, that much more enjoyable.

I would also like to thank Henk van der Meer and Thony van der Gon Netscher for their availability.

Finally, I thank all my friends and family for their moral support.

Appendix

1. Averaged trend lines

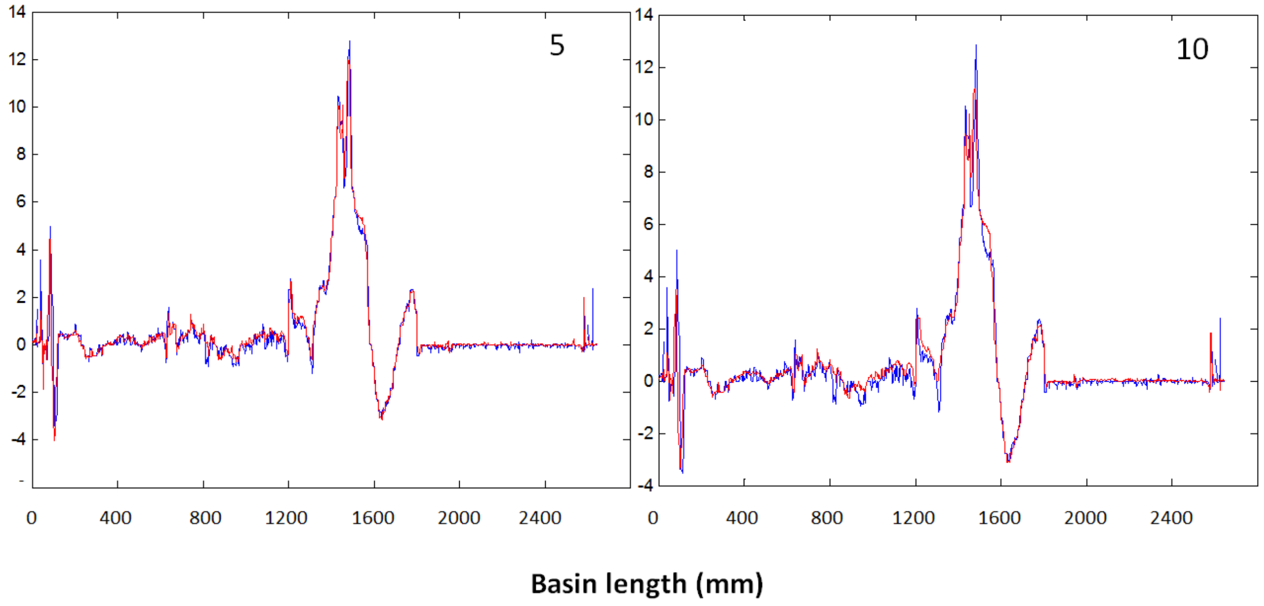

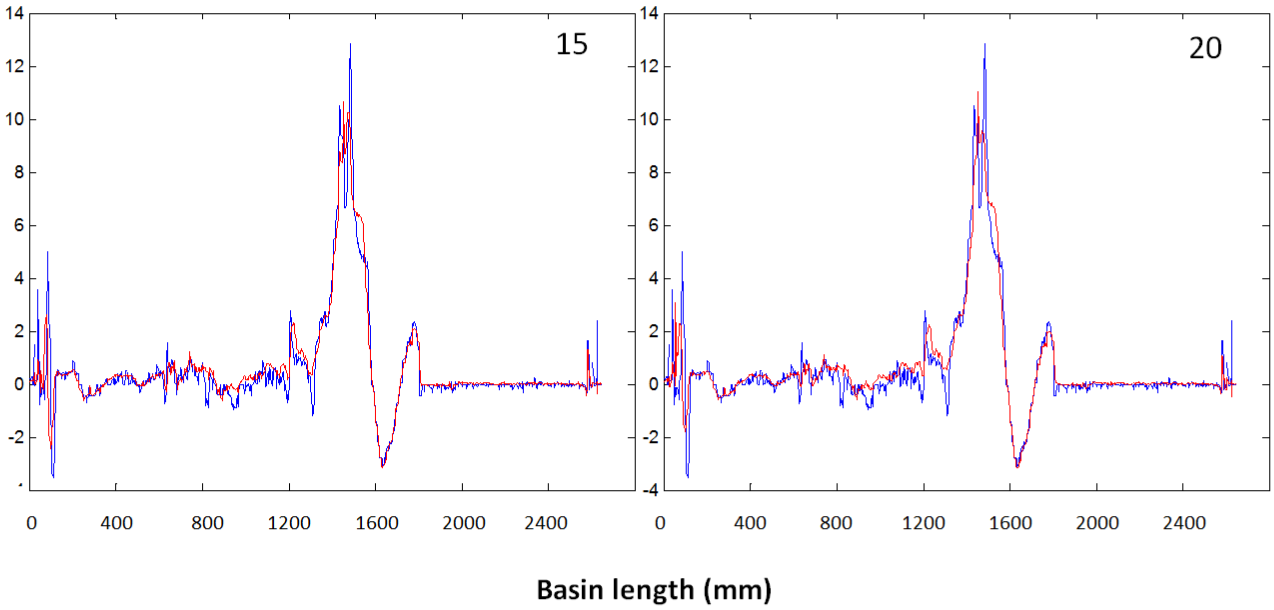

By averaging different width of trend line, a smoother curve was obtained. For that, a number of averages were compared to find the best trend line, which would keep the general information of the line but also remove the sharp peaks. The number of transect line used are shown in the upper right corner of each graph. The blue line represents a single transect line, and the red line represents the averaged trend lines. 15 averaged transect lines were used in this research.

2. Changes in sedimentation along the basin length

During basin filling, deposition was not linear so instead of using the last topographic scan as the local long-term sedimentation rate, the next topographic scan of the local sedimentation rate was used in order to follow as precisely as possible the deposition trend. Analyses of the long-term sedimentation rate at any one transect location reveals a record composed of periods of stasis, erosion and deposition. The average value of all local-long term sedimentation rate was used to determine how deposition varied with time in order to determine the best value that would disregard the effect of erosion. The period of erosion appear to increase as we move downstream, the period of stasis are mostly upstream during SLR and the period of deposition are mostly upstream with no sea-level changes and upstream of SLF. We decided to remove all values of average local long-term sedimentation rate that were below 0.03 in EXP1 and below 1.0 during SLF and 0.03 during SLR in EXP2.

EXP1- B1

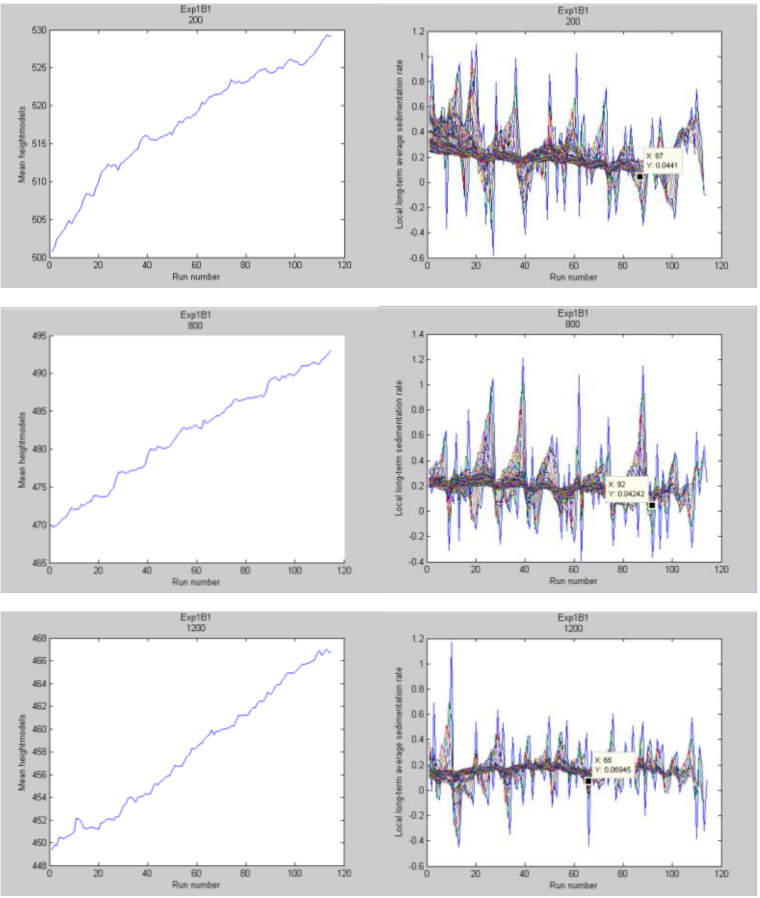

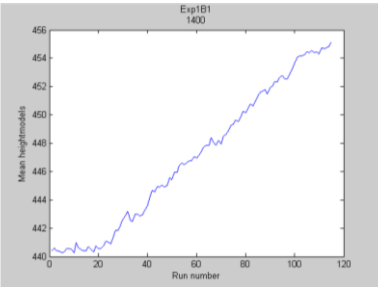
Exp1B1
1400
Mean heightmodels
Run number

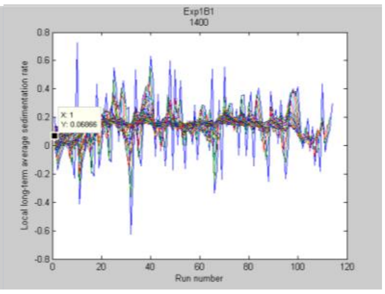
Exp1B1
1400
Local long-term average sedimentation rate
Run number
X: 1
Y: 0.06866

EXP1-B2

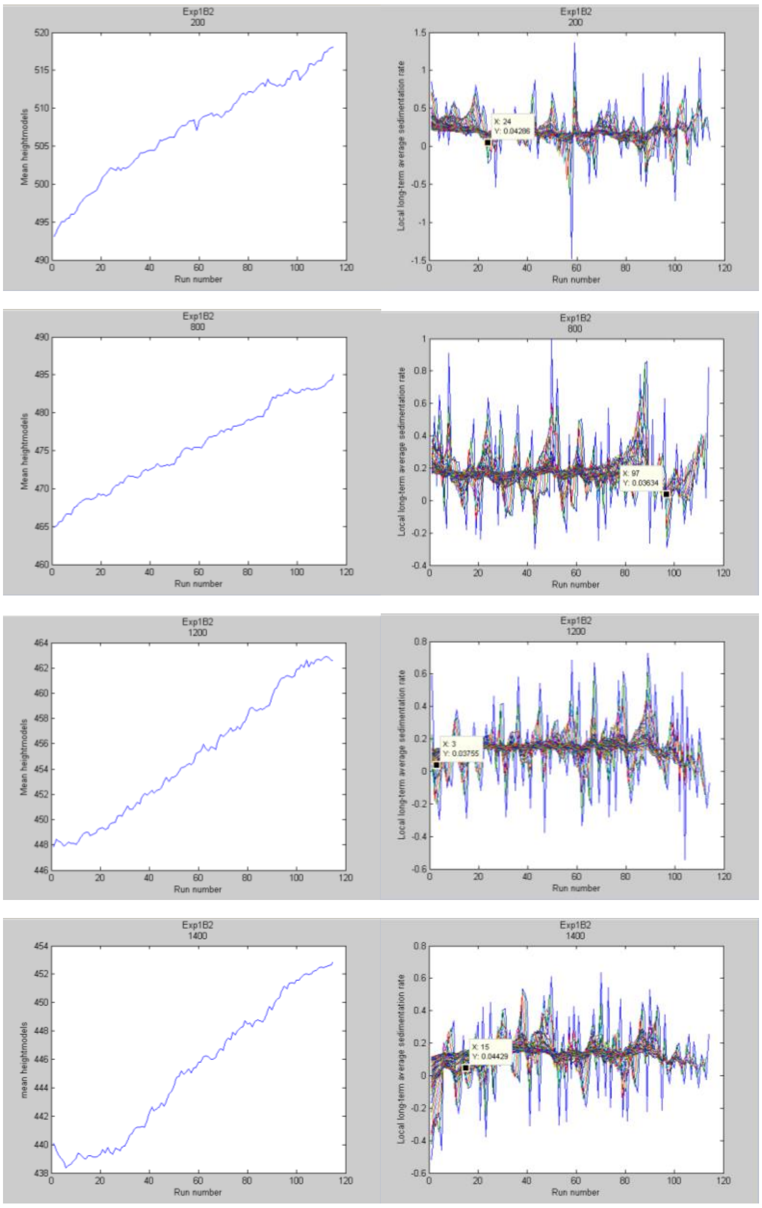

Exp1B2
200
Mean heightmodels
Run number
Exp1B2
200
Local long-term average sedimentation rate
Run number
X: 24
Y: 0.04286
Exp1B2
800
Mean heightmodels
Run number
Exp1B2
800
Local long-term average sedimentation rate
Run number
X: 97
Y: 0.03634
Exp1B2
1200
Mean heightmodels
Run number
Exp1B2
1200
Local long-term average sedimentation rate
Run number
X: 3
Y: 0.03755
Exp1B2
1400
mean heightmodels
Run number
Exp1B2
1400
Local long-term average sedimentation rate
Run number
X: 15
Y: 0.04429

EXP2 B1 SLR

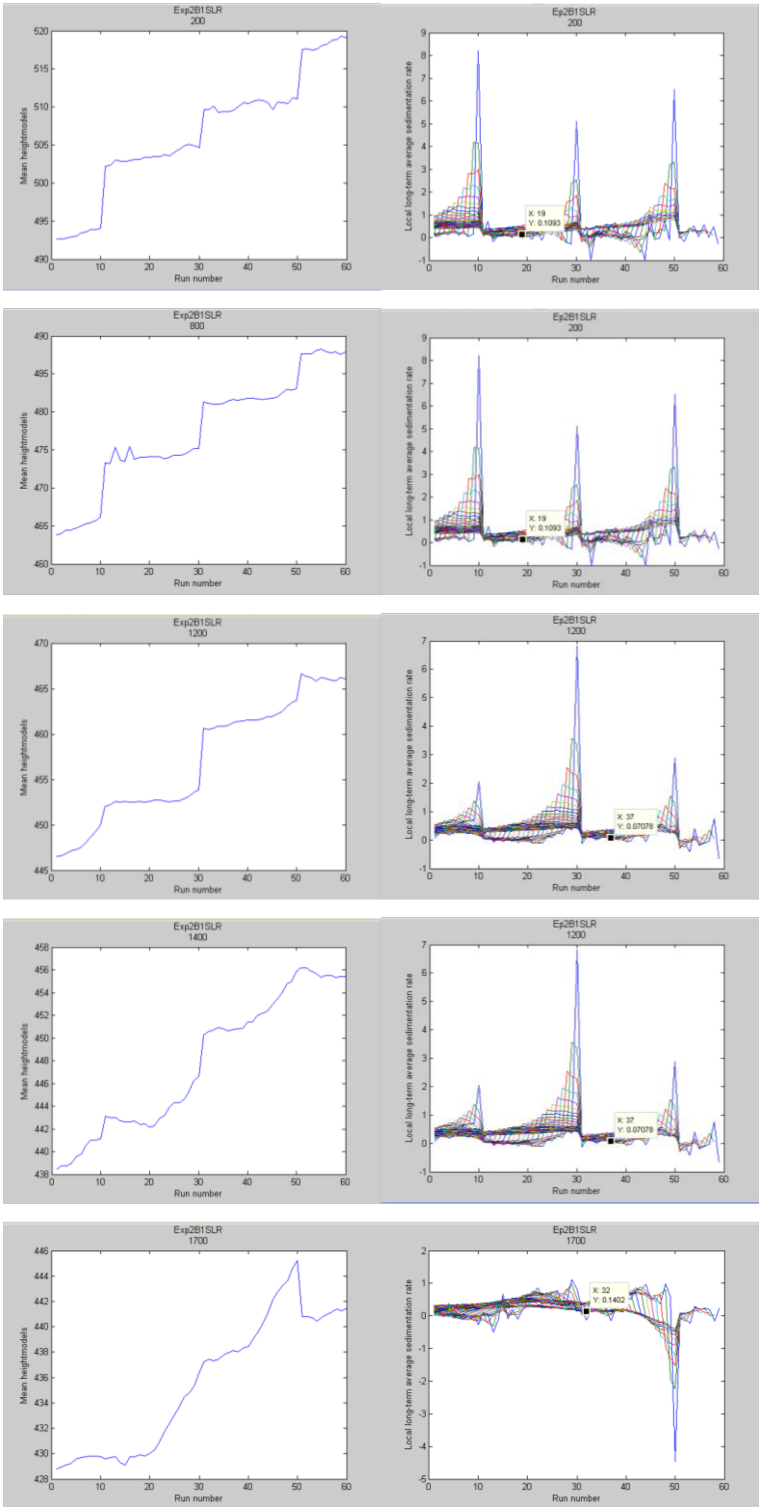
Exp2B1SLR
200
Mean heightmodels
Run number
Ep2B1SLR
200
Local long-term average sedimentation rate
X: 19
Y: 0.1093
Exp2B1SLR
800
Ep2B1SLR
200
Exp2B1SLR
1200
Ep2B1SLR
1200
X: 37
Y: 0.07078
Exp2B1SLR
1400
Ep2B1SLR
1200
Exp2B1SLR
1700
Ep2B1SLR
1700
X: 32
Y: 0.1402

EXP2 B1 SLF

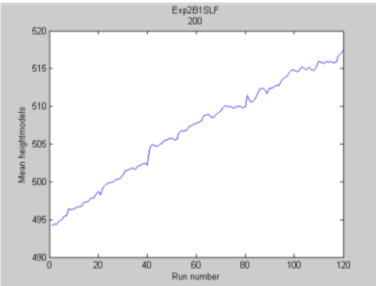
Exp2B1SLF
200
Mean heightmodels
Run number

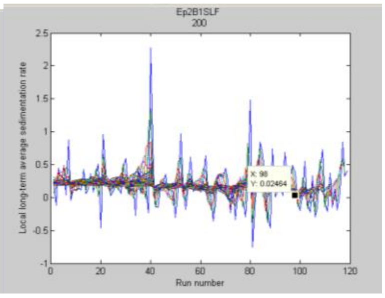
Ep2B1SLF
200
Local long-term average sedimentation rate
Run number

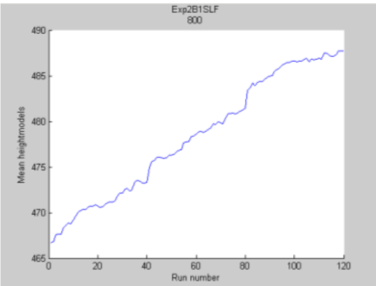
Exp2B1SLF
800
Mean heightmodels
Run number

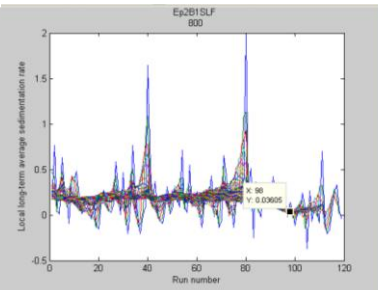
Ep2B1SLF
800
Local long-term average sedimentation rate
Run number

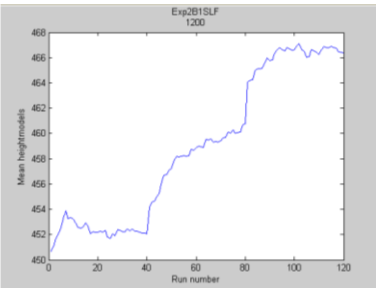
Exp2B1SLF
1200
Mean heightmodels
Run number

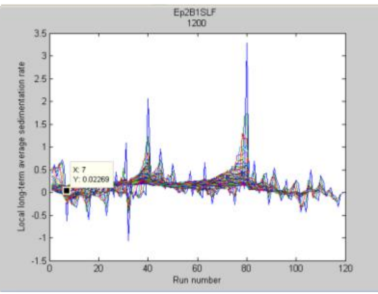
Ep2B1SLF
1200
Local long-term average sedimentation rate
Run number

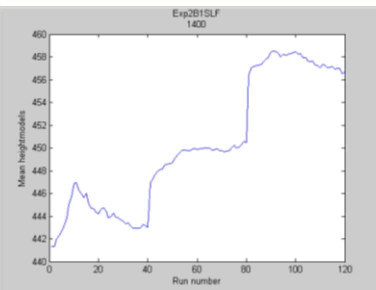
Exp2B1SLF
1400
Mean heightmodels
Run number

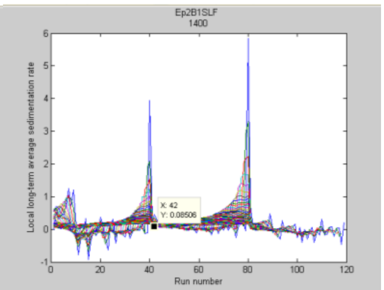
Ep2B1SLF
1400
Local long-term average sedimentation rate
Run number

EXP2 B2 SLR

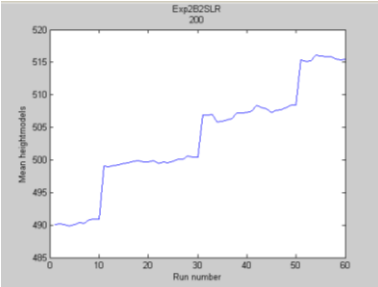
Exp2B2SLR
200
Mean heightmodels
Run number

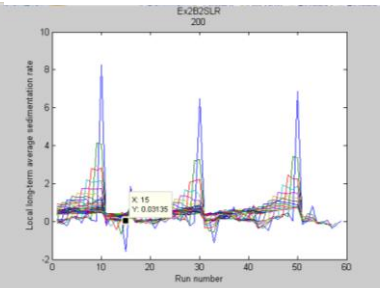
Ex2B2SLR
200
Local long-term average sedimentation rate
X: 15
Y: 0.03135
Run number

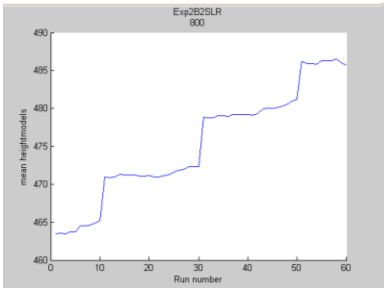
Exp2B2SLR
800
mean heightmodels
Run number

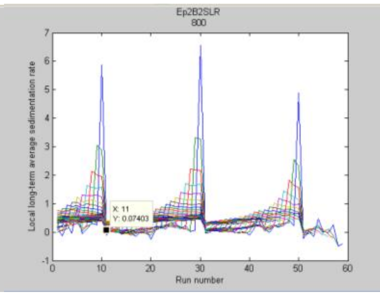
Ep2B2SLR
800
Local long-term average sedimentation rate
X: 11
Y: 0.07403
Run number

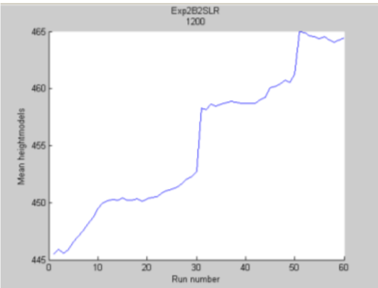
Exp2B2SLR
1200
Mean heightmodels
Run number

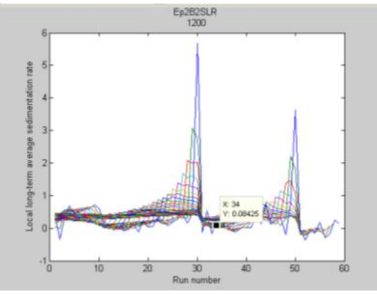
Ep2B2SLR
1200
Local long-term average sedimentation rate
X: 34
Y: 0.08425
Run number

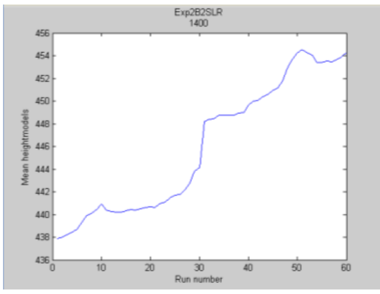
Exp2B2SLR
1400
Mean heightmodels
Run number

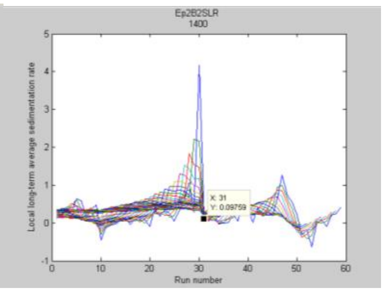
Ep2B2SLR
1400
Local long-term average sedimentation rate
X: 31
Y: 0.09759
Run number

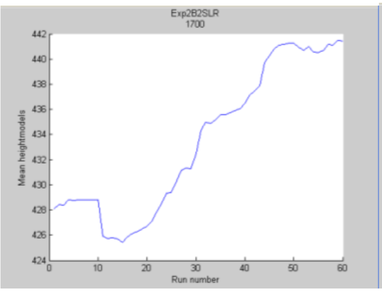
Exp2B2SLR
1700
Mean heightmodels
Run number

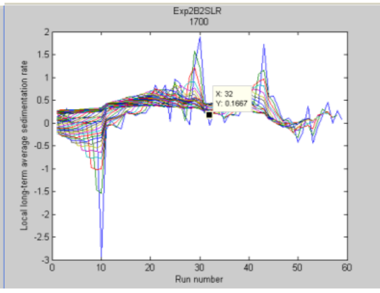
Exp2B2SLR
1700
Local long-term average sedimentation rate
X: 32
Y: 0.1667
Run number

EXP2 B2 SLF

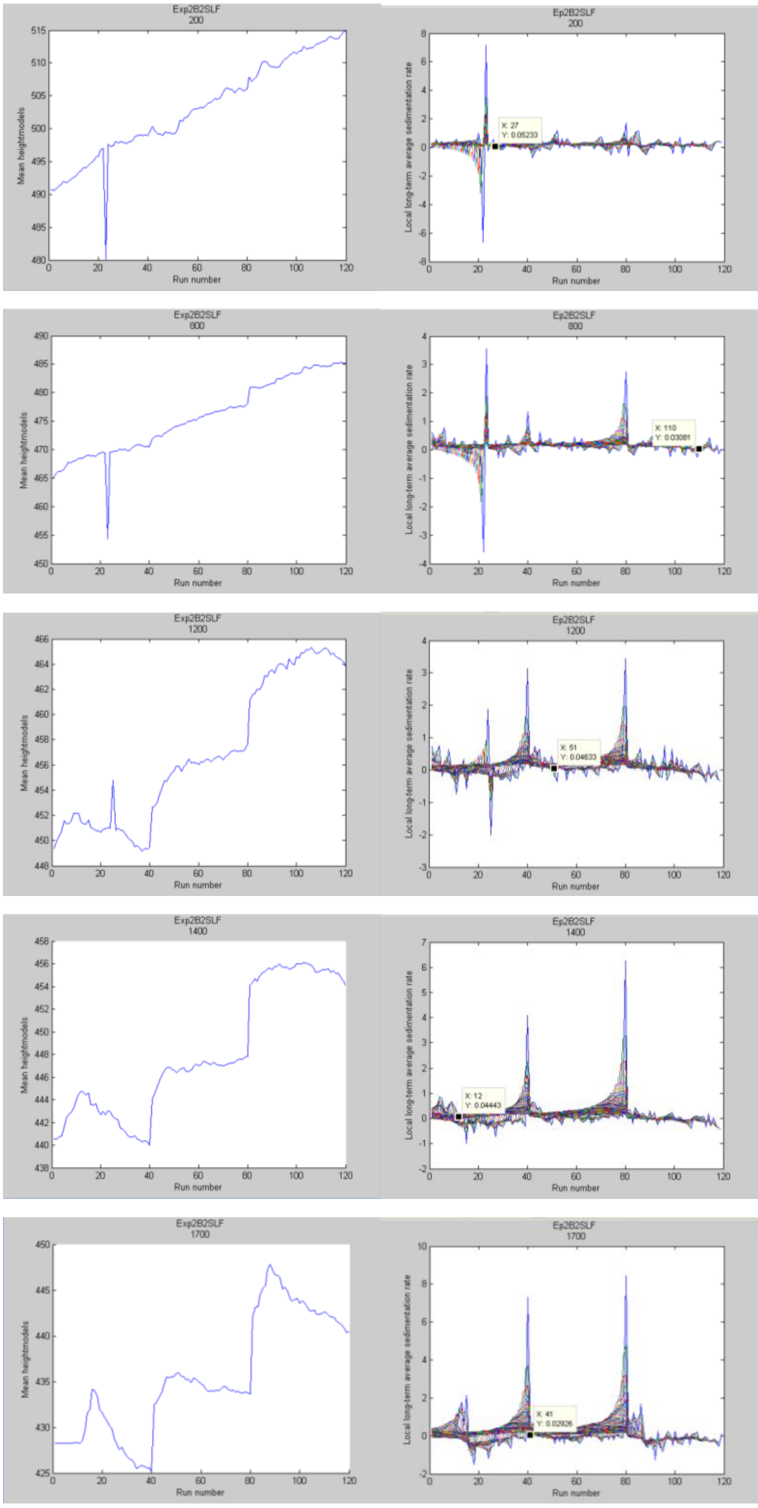

Exp2B2SLF
200
Mean heightmodels
Run number
Ep2B2SLF
200
Local long-term average sedimentation rate
X: 27
Y: 0.05233
Exp2B2SLF
800
Ep2B2SLF
800
X: 110
Y: 0.03081
Exp2B2SLF
1200
Ep2B2SLF
1200
X: 51
Y: 0.04633
Exp2B2SLF
1400
Ep2B2SLF
1400
X: 12
Y: 0.04443
Exp2B2SLF
1700
Ep2B2SLF
1700
X: 41
Y: 0.02926

3. Cutoff values

In order to further optimize our results, a cutoff value of 10000 was used as it is pure outlier. After removing all outliers of 10.000 and more, all values larger than 10-fold the standard deviation were removed.

EXP-B1

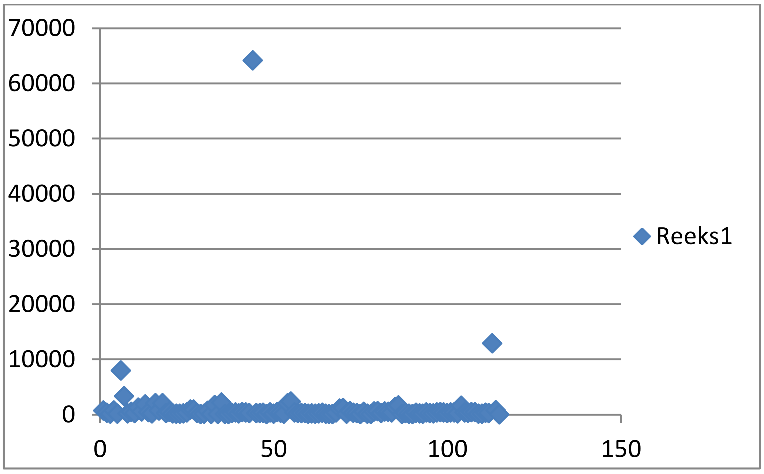

EXP1-B2